

AD-A220 265

ATION PAGE

Form Approved
OMB No 0704 0188



Pub
gait
coll:
Dav

verage 1 hour per response, including the time for reviewing instructions, searching existing data sources, the collection of information, send comments regarding this burden estimate or any other aspect of this Washington Headquarters Services, Directorate for Information Operations and Reports, 1215 Jefferson Management and Budget, Paperwork Reduction Project (0704-0188), Washington, DC 20503

1. AGENCY USE ONLY (Leave blank)		2. REPORT DATE 3/31/90	3. REPORT TYPE AND DATES COVERED Final Report	
4. TITLE AND SUBTITLE CVD Diamond Films for Tribological Applications			5. FUNDING NUMBERS C N00014-89-C-0151 PE 63220 P S405018 TA SRT WU 01	
6. AUTHOR(S) Linda S. Plano			8. PERFORMING ORGANIZATION REPORT NUMBER	
7. PERFORMING ORGANIZATION NAME(S) AND ADDRESS(ES) Crystallume 125 Constitution Drive Menlo Park, CA 94025			10. SPONSORING/MONITORING AGENCY REPORT NUMBER	
9. SPONSORING/MONITORING AGENCY NAME(S) AND ADDRESS(ES) SDIO/1ST ONR, Code 1114 Arlington, VA 22217			10. SPONSORING/MONITORING AGENCY REPORT NUMBER N/A	
11. SUPPLEMENTARY NOTES 				
12a. DISTRIBUTION/AVAILABILITY STATEMENT Approved for public release; distribution unlimited			12b. DISTRIBUTION CODE N/A	
13. ABSTRACT (Maximum 200 words) Friction and wear behavior of several types of diamond film has been studied using sapphire on diamond film and diamond on diamond film tests. The coefficient of friction of the films was found to be a strong function of film morphology for sapphire on diamond film tests, and of diamond bonding content for diamond on diamond film tests. Smooth films were found to have coefficients of friction approaching the lower value for natural diamond on natural diamond (0.05), regardless of bonding composition. Films were deposited in three groups. Film morphology and graphite content were varied in the first group. In the second group, increased growth rates of highly diamond-bonded material were sought. Smooth, very fine grained material of varied bonding content was produced in the third. Attempts at surface planarization through etching and regrowth were not successful. All films were found to have excellent adhesion to both silicon and silicon carbide substrates. This study indicates that CVD diamond films have excellent potential for use as solid-film bearings, and that this potential merits further work.				
14. SUBJECT TERMS Friction, wear, PECVD Diamond film			15. NUMBER OF PAGES 46	
17. SECURITY CLASSIFICATION OF REPORT UNCLAS			16. PRICE CODE	
18. SECURITY CLASSIFICATION OF THIS PAGE UNCLAS		19. SECURITY CLASSIFICATION OF ABSTRACT UNCLAS		20. LIMITATION OF ABSTRACT SAR

SDIO/ N00014-89-C-0151

CVD DIAMOND FILMS FOR TRIBOLOGICAL APPLICATIONS

LINDA PLANO

PRINCIPAL INVESTIGATOR
CRYSTALLUME
MENLO PARK, CA

IAN HAYWARD AND JOHN WEGAND
GEO-CENTERS
FORT WASHINGTON, MD
(currently working under contract at Naval Research Laboratory)

Application For	
NTIS	<input checked="" type="checkbox"/>
DTIC	<input type="checkbox"/>
ERIC	<input type="checkbox"/>
Other	<input type="checkbox"/>
By _____	
Distribution _____	
Availability _____	

Dist	Special
A-1	

MARCH 31, 1990

90 04 00 013

CVD DIAMOND FILMS FOR TRIBOLOGICAL APPLICATIONS

Contract No. N00014-89-C-0151

Final Report
March 30, 1990

LINDA PLANO, IAN HAYWARD, AND JOHN WEGAND

PROJECT SUMMARY

Natural diamond and high pressure/ high temperature (HPHT) synthesized diamond have been used in some friction and wear applications, such as tool coatings, because of diamond's extreme hardness. Its low coefficient of friction (0.05 for diamond on diamond in dry air, similar to that of Teflon) is a property rarely remembered and little used. The advent of diamond film as a routine engineering material suggests that diamond may significantly benefit friction and wear applications.

Diamond films have been deposited by plasma enhanced chemical vapor deposition (PECVD) by researchers throughout the world. The extent to which this material's properties can be controlled by the deposition technology indicates that it will be possible to overcome the drawbacks of natural diamond (high cost, inflexible morphology) while maintaining its useful properties.

Selected films have been shown to exhibit coefficients of friction approaching that of natural diamond or Teflon. Wear rates for certain morphologies were found to be relatively low. Initial surface morphology appears to be the strongest determinant of tribological behavior while neither ambient humidity nor, surprisingly, extent of diamond bonding appears to have a strong effect.

Tribological behavior of polycrystalline materials is inherently difficult to interpret because of chemical and mechanical effects. The problem is exacerbated in the case of multiple-phase materials, such as diamond film, which can contain sp^2 and sp^1 bonding as well as sp^3 (diamond) bonding. In addition, diamond films are so hard and, often, so abrasive that it is difficult to maintain testing apparatus in the condition necessary to obtain useful data. However, it is possible to determine some basic tribological characteristics of various types of diamond films through standard techniques, such as pin-on-disk and reciprocating sliding tests.

Diamond films were deposited using either microwave or DC excited plasmas and a variety of deposition conditions. Major variables included substrate temperature, substrate material, gas mixture, and precursor gas identity. Film morphologies ranged from predominantly mixed (100) and (110) facets to predominantly (111) and included cauliflower type growth. Raman spectroscopy of the films indicated a range from purely diamond-bonded to highly defective, graphitic material that probably also included a large percentage of hydrogen.

Fine-grained films were found to display the most desirable tribological characteristics, regardless of bonding type. Predominantly (100)/(110) surfaced films also appeared to have better characteristics than other types of films. Diamondlike carbon films tended to interact severely with the testing stylus, greatly complicating analysis.

The results given above indicate that for maximum lifetime with minimum wear to the opposing face, a product should be coated with diamond of as smooth a surface as possible. If some nondiamond-bonded material must be allowed into the film to achieve a smooth surface, it should be an acceptable compromise. However, it is probably possible to deposit purely diamond-bonded material of an acceptable smoothness. For applications requiring significant wear of the opposing surface (e.g., for tool bits), it is not clear whether a rough surface or a smooth surface deposited on a substrate machined for optimum cutting capability is preferred. Such analysis requires further testing.

The data developed in this study indicate excellent potential for CVD diamond use in tribological applications. Extension of diamond film to a variety of tribologically related end uses, such as bearings, tooling, and protective coatings against erosion, appears warranted.

I. INTRODUCTION

1.1 General Information

Natural diamond and high pressure, high temperature (HPHT) synthesized diamond have found widespread use as industrial abrasives. Individual crystals are used for cutting, milling, and turning applications while smaller particles are used, bonded in a matrix or in loose form, for grinding applications. Diamond also exhibits a very low coefficient of friction in air, a property that has not been extensively exploited because of the expense of developing large area surfaces from individual crystals.

Tools coated with diamond in a matrix are more common than those consisting of a single diamond crystal. The ability to coat tools with contiguous diamond film would represent a significant improvement over those coated with the bonded material since the properties of interest would not be affected by the presence of matrix material. In addition, if the morphological characteristics of the film could be tailored to the application, e.g., smooth for precise cutting, rough for abrading, the utilization of diamond as an industrial abrasive could greatly increase.

Until recently, diamond was available only in its natural form or in particulate form from high pressure, high temperature (HPHT) synthesis. The development of enhanced CVD methods for the deposition of polycrystalline (and eventually single crystal) diamond films presents a simpler and potentially more economical method of coating tools. The ability to manipulate film morphology and bonding content allows the film to be made as abrasive or as smooth as the application requires. An additional asset is that, because diamond is the best room temperature thermal conductor, it may allow the use of much higher tool feed rates since heat dissipation can be maximized. And, as discussed in an earlier report, diamond films may be useful in preventing oxidation of low temperature-oxidizing materials [1]. Values for properties important to tribological applications are compared with other engineering materials in Tables 1 through 4.

Currently it is not possible to grow single crystal diamond on nondiamond substrates. Nonetheless, it may be possible to approximate the single crystal ideal through one of several methods, including (1) growth of fine grained material and (2) smoothing of a rough diamond film surface by either *in situ* or *ex situ* techniques. Experimental evidence to date suggests that growth of fine-grained material is currently the most effective method of producing low friction, low wear diamond films.

Table 1. Young's Moduli of diamond and selected materials (Units : 10^{11} N/m²)

Diamond	10.35
Silicon Carbide	7.0
Silicon Nitride	1.6- 3.85
Silicon	1.9
Boron Nitride	1.5 - 2.5

Table 2. Hardness of diamond and selected materials (Units : 10^6 kg/m²)

Diamond	9000
Cubic Boron Nitride	4500
Titanium Nitride	3000
Silicon Carbide	2500
Tungsten Carbide	1900

Table 3. Thermal conductivity of diamond and selected materials (Units : 10^2 W/m-K)

Natural Diamond	20.0
CVD Diamond Films	12.0 -18.0
Copper	4.0
Graphite	2.1
Silicon Carbide	2.7
Aluminum Nitride	1.7
Aluminum Oxide	0.4

The possibility of synthesizing high quality diamond films on various structural materials permits an improvement of the properties of these materials through enhancing their wear resistance and reducing their coefficient of friction. In addition, the exceptional thermal conductivity of diamond improves thermal performance of surfaces by enhancing their heat spreading and heat dissipation characteristics, thus minimizing the component temperatures

In Phase I of this program the tribological characteristics of CVD diamond films have been investigated in order to determine effects of morphology and diamond bonding on film friction and wear. All films were prepared at Crystallume, where they were analyzed for bonding type, morphology, and adhesion. Tribological tests were performed by Hayward and Wegand of NRL.

Two types of tests were performed: reciprocating sliding and pin-on-disk. The former utilizes a sapphire stylus while the latter incorporates a diamond stylus.

The remainder of this section will be used to introduce basic data on diamond and graphite oxidation, and on diamond film nucleation and growth.

A summary of the results of the tribological tests follows:

Diamond deposition:

- The addition of carbon monoxide to the precursor mix increases deposition rate, but can also lead to an increase in incorporated nondiamond bonded material in the grain boundaries. Low growth rates are obtained if the grain boundary problem is minimized.

Reciprocating sliding tests:

- Sapphire stylus wear increases with increasing initial film roughness.
- Initial surface morphology appears to be the strongest determinant of initial friction values.
- In the range studied, humidity had no observable effect on friction behavior.

Pin-on-Disk tests:

- Minimum friction approaches that of natural diamond (0.05) regardless of film morphology or diamond content.
- Initial friction shows some dependence on surface roughness, but more data are needed.
- Initial friction is also a function of film diamond bonding content.
- Humidity had no strong effect on these tribological tests either.

Table 4. Coefficient of Friction (dry) of diamond and selected materials.

Diamond on Diamond	0.05
Sapphire on Sapphire	0.2
Graphite on Graphite	0.1
Tungsten Carbide on Tungsten Carbide	0.17

1.2 Tribological Behavior of Natural Diamond

Friction has two main components, one due to surface roughness, the other to adhesion. Typically, smoother surfaces have higher adhesion (in part because of the large contact area) than rougher surfaces do, so determining a low friction film requires optimizing these two parameters, as indicated by the schematic graph in Figure 1.

Diamond is rough on a 5 nm scale, even after polishing. One result of this roughness is that adhesion is generally very low under most conditions. However, if a diamond crystal is cleaved in vacuum, adhesion and friction are strongly increased [2]. If air is then admitted to the new surface, friction decreases to its original level. The reason for this behavior is the existence of a noncarbon layer of atoms that rapidly attach to the dangling bonds present on the newly cleaved diamond surface [3]. Without this layer, the dangling bonds attempt to bond with other reactive surfaces, greatly increasing friction due to adhesion. When friction tests are performed in air, the dangling bonds are so rapidly satisfied with contaminant atoms that, in general, no effect is seen. If sufficient rubbing is performed at a high enough rate, the contaminant layer can be worn off, also resulting in increased friction. Without the contaminant layer, the upper atomic layers reconstruct to graphite [3].

Friction in diamond is dependent on crystal orientation and rubbing direction. The mechanically hard face of diamond, (111), is also the one with the lowest coefficient of friction: 0.05 in dry air. No significant anisotropy is observed in this coefficient. The (100) face exhibits coefficients of friction from 0.05 to 0.15, depending on the direction of rubbing.

Friction between two natural diamonds is not greatly affected by the addition of a lubricant.

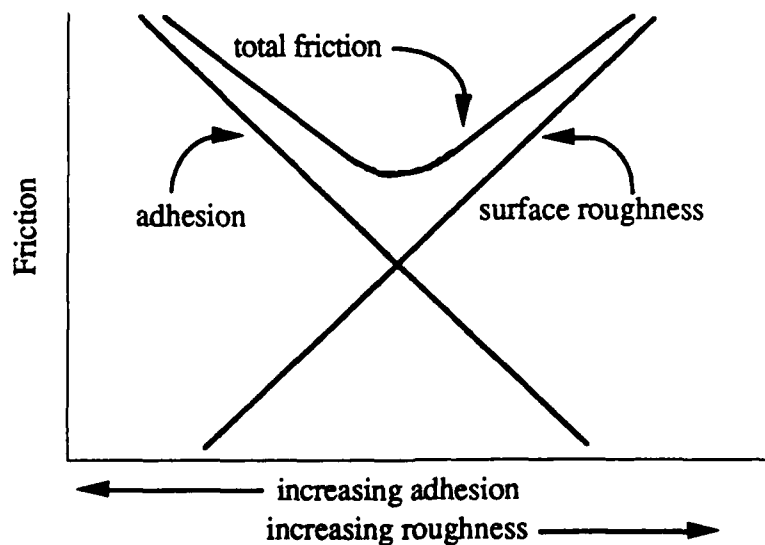


Figure 1: Effects of adhesion and surface roughness on total friction.

1.3 Diamond Film Nucleation and Growth

PECVD diamond films are routinely deposited by researchers throughout the world [4,5,6]. Plasma enhanced, torch, and hot filament techniques are the most commonly used deposition techniques. Plasma excitation is most commonly by microwave. Several diamond precursors have been studied, including methane, acetylene, carbon monoxide, and several alcohols. Methane remains the most common precursor, although carbon monoxide, oxygen, and water are in extensive use, usually as additives. The most common substrate is silicon, although a variety of substrates has been explored at Crystallume, including molybdenum, titanium, copper, and quartz. Typical deposition temperatures range from a low of 300 °C up to ~ 1000 °C while pressures vary from less than a torr to atmospheric pressure. Clearly, diamond deposition is a versatile process. However, successful development of applications is more difficult than simple diamond crystallite formation since products require uniform films over significant substrate areas.

Thin film structure, in general, is highly dependent on the nature of the substrate surface since the surface influences adsorption, mobility, and chemisorption of reactant species. These influence the size of the critical nucleus, upon which the orientation and morphology of the subsequent grain is based. Therefore, by controlling film nucleation, one can strongly influence the structure of the final film. Different *in situ* nucleation techniques, some developed at Crystallume, are used to insure the deposition of reproducible films.

Diamond film growth is affected by variables such as temperature, pressure, carbon precursor concentration, and plasma conditions. The use of these variables for control of film characteristics is most useful after nucleation has been established. If nucleation rate is increased, the effect of process variables on nucleation can be more effectively studied and exploited. The most frequently employed nucleation technique is abrasion of the substrate with diamond dust so as to provide a high density of energetically favorable nucleation sites [7,8]. The primary drawback to this type of nucleation enhancement is that the process of abrasion is difficult to control reproducibly.

Once nucleation has been established, rapid diamond growth can occur. Grain size can be affected by the nucleation enhancement process, but other deposition parameters, such as substrate temperature and plasma power density, are more influential. The most important role of nucleation enhancement appears to be that of causing a film, rather than isolated particles, to form.

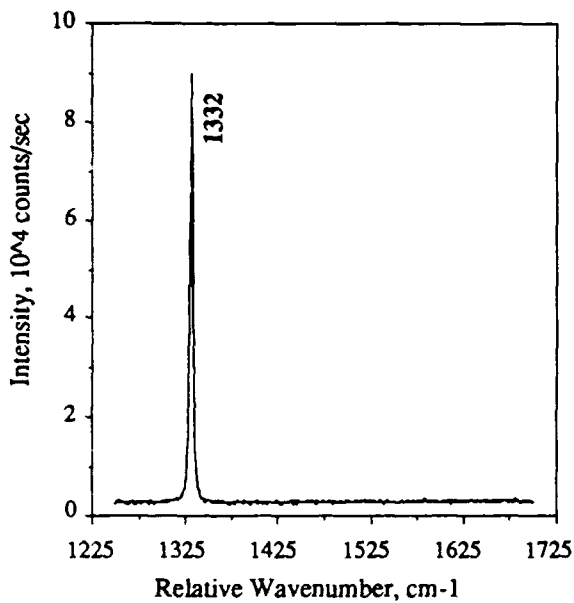
1.4 Diamond Film Characterization

Two of the most important characteristics of a diamond film are the extent of diamond bonding (as opposed to graphitic or hydrocarbon bonding) and its overall morphology. By far the most commonly used and sensitive technique for the former measurement is Raman spectroscopy. SEM is most commonly used for surface morphology and film thickness.

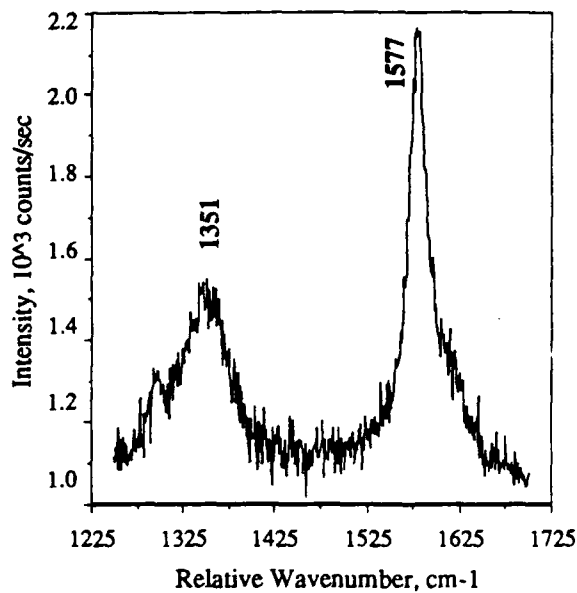
Since Raman spectroscopy is a less well known characterization technique, a brief description is included here. The Raman spectrometer detects bonding type by measuring wavelength-shifted light produced through Raman scattering from a sample that has been illuminated with an argon laser. The magnitude of the wavelength shift is characteristic of the type of bonding present in the sample. This technique is superior to more traditional analytical methods, such as X-ray diffraction, for characterization of diamond films for several reasons. First, it is the only readily applicable method which provides an indication of carbon bonding state throughout the bulk of a sample, rather than only at the surface. Second, the spot size is small, on the order of 1 to 500 μm , allowing differentiation between closely spaced points of interest. Third, very thin films (on the order of $\sim 0.2 \mu\text{m}$) are sufficient to yield useful spectra. Finally, it is a nondestructive technique.

Raman spectra of polycrystalline graphite, natural diamond powder, polycrystalline diamond film, and diamondlike carbon (DLC) are shown in Figure 2. These spectra clearly demonstrate the utility of the Raman technique in the differentiation of the various bonding states of carbon. The diamond peak is at approximately 1333 cm^{-1} [9]. Graphite peaks can exist in several locations [10]. Pure crystalline graphite can have a peak at 1580 to 1600 cm^{-1} , depending on the preparation method. Defects cause different Raman shifts, with, for example, in-plane defects causing a peak at 1350 - 1370 cm^{-1} , according to Tuinstra, et al [11]. Other peaks have not been definitively identified, but are thought to be due to defects in sp^2 bonded carbon. Raman analysis is approximately 100 times more sensitive to graphite bonding than to diamond (depending on the wavelength of the exciting radiation) [12] making this a superior technique for identifying even very small amounts of graphite in a primarily diamond film.

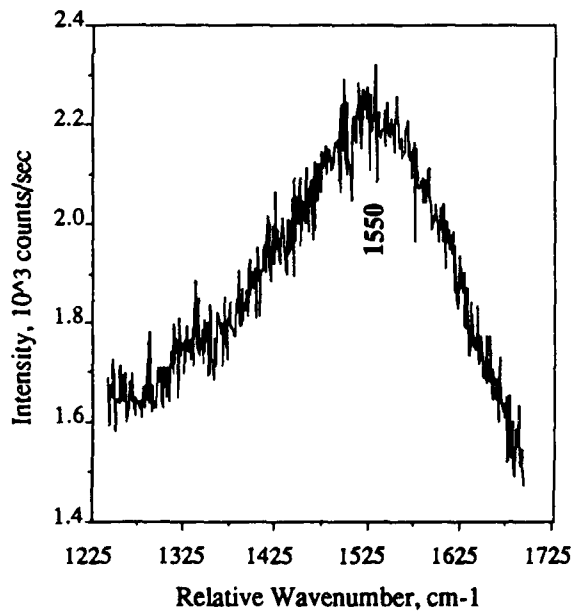
A useful measure of the extent of diamond bonding in a carbon film can be achieved by taking the ratio of peak intensities of diamond (1332 cm^{-1}) and nondiamond bonded carbon (typically graphite at $1580 - 1600 \text{ cm}^{-1}$ or "amorphous" carbon at $\sim 1500 \text{ cm}^{-1}$). The sp^3/sp^2 ratio is plotted as a function of methane concentration in the reactant gas mix in Figure 3 (these results are for DC-excited plasmas). The curve indicates that lower methane concentrations yield more diamond and less graphitic bonding than do higher methane concentrations, a relationship confirmed by extensive experimental data.



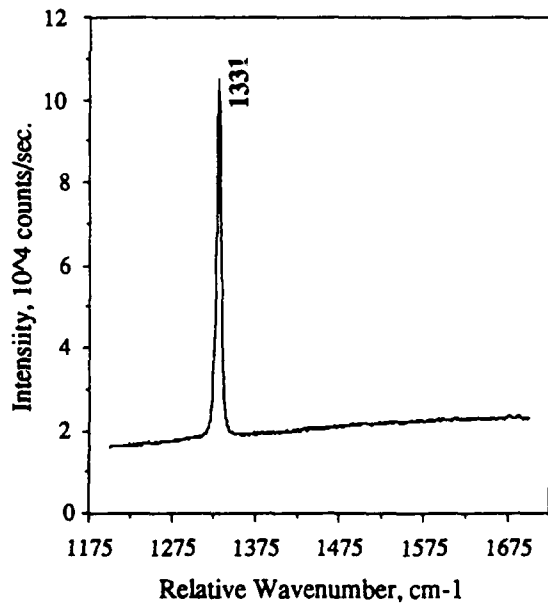
(a)



(b)



(c)



(d)

Figure 2: Raman spectra for (a) natural diamond, (b) pyrolytic graphite (HPOG), (c) ion beam deposited diamondlike carbon (DLC), and (d) diamond film.

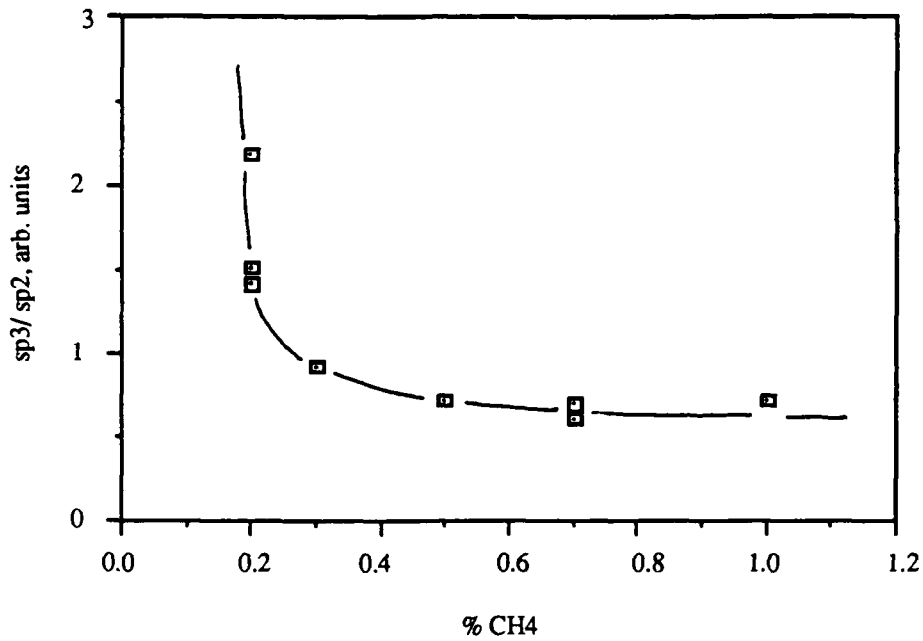


Figure 3: Diamond (sp^3) to graphite (sp^2) bonding ratio in diamond films deposited using different methane concentrations in the reactant gas mixture. Bonding type was determined by Raman spectroscopy.

II. EXPERIMENTAL WORK

Experimental work consisted of diamond film deposition and characterization performed at Crystallume followed by tribological testing at NRL. The experimental details of each facet of the research are discussed in the next two sections.

2.1 Diamond Film Growth

Diamond films were deposited in three groups. Deposition parameters were varied within each group to attain a goal specific to that group. In the first group, a variety of morphologies and graphite contents were generated so that their effects on the resulting films could be observed. Relative concentrations of carbon monoxide and methane was the primary variables studied. The goal of the second group was to attain maximum deposition rates without sacrificing diamond bonding in the films. This group was deposited while preliminary tribology measurements were being made at NRL. Measurement results indicated that fine-grained films would be of interest, so the third and final group focussed on the deposition of this type of material. Films from the first and third groups were used for tribological analysis while the second was used for deposit optimization.

In the first group (Group A), all diamond film depositions were performed under equivalent plasma, substrate, pressure, and gas flow rate conditions. Microwave excitation was employed. Nominal values of the deposition parameters were 900 W, 70 torr, and 35 sccm, respectively. The relative amount of carbon precursors in hydrogen was varied between 0 - 3% (for up to a total of 6% carbon-containing gases), as was the temperature (700 - 800 °C). High purity methane (99.9995 %) and carbon monoxide (99.997 %) were used in combination and separately. These depositions were performed on 2" silicon substrates prepared for film nucleation by scratching with 0.1 μm diamond dust. One set of conditions was repeated on a silicon carbide substrate, also scratched with diamond dust.

The second group of films (Group B) was deposited under conditions similar to those given above, but with a microwave power of 1000 W, total reactant gas flow rate of 200 sccm, and total pressure of 75 torr. Increased power leads to a higher density of excited species, especially atomic hydrogen, which are critical for diamond growth. Higher flowrates and pressures are expected to maximize the flow of reactants to the substrate surface (assuming flowrate remains below the level of significant boundary layer formation). These changes were expected to result in increased diamond growth rate and improved ratio of diamond to nondiamond-bonded carbon in the films, both important factors in developing diamond films for certain tribological applications.

For the third group of films (Group C), deposition parameters were set to previously defined conditions that are known to produce fine-grained material. Low substrate temperatures and reduced growth rate both appear to be important in producing this material. These films were deposited uniformly across 2 and 4 inch substrates. Three films (two on silicon, one on silicon carbide) were grown at low temperature (~500 °C) in a microwave reactor while the remaining film was grown in a DC reactor.

An *in situ* method of surface smoothing was performed. Selected diamond films were subjected to hydrogen plasma etch in an attempt to remove asperities. The etch was followed by a new cycle of nucleation and growth to determine whether the new nucleation would force smaller grain size.

Each film was analyzed for bonding type and morphology by Raman spectroscopy and SEM, respectively. Selected films were tested for adhesion by applying, then rapidly removing, transparent tape to the film surface.

2.2 Tribological Tests

Surface roughness of selected films was estimated with an Alpha Step profilometer. The center line average (CLA) was used as the measure of roughness. CLA is calculated as follows:

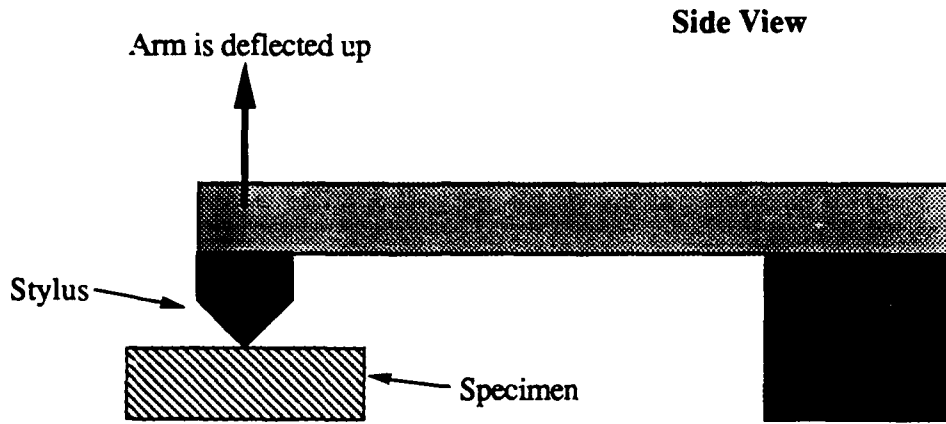
$$\text{CLA} = \frac{\sum_{i=1}^N (y_i - \langle y \rangle)}{N}$$

where y_i represents the distance from the center line to peak or valley.

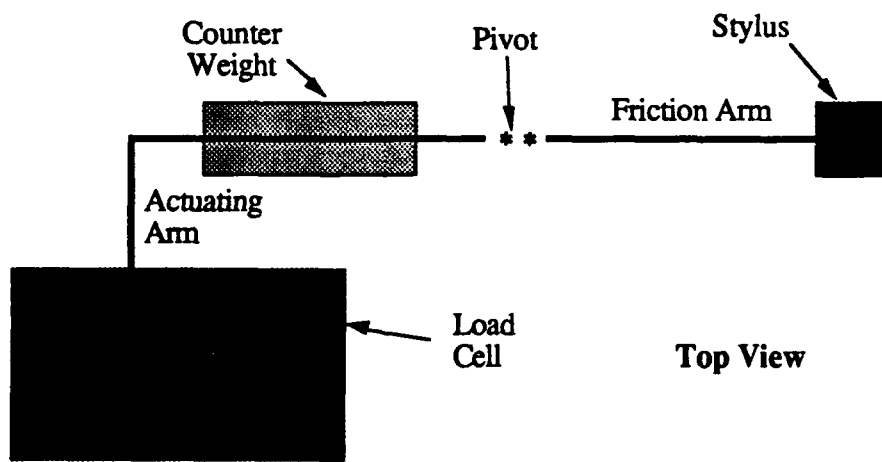
All tribological tests were performed at NRL by Ian Hayward and John Wegand. Two types of friction tester were employed: reciprocal sliding, in which a sapphire ball was employed as the wearing surface, and pin-on-disk, which utilizes a diamond stylus.

In the case of the reciprocating sliding measurements, lateral and vertical strain gauges on the stylus support arm are used to monitor friction behavior. Normal force is applied *via* a cantilever, as illustrated by the schematic diagram in Figure 4a. The sample was moved back and forth along a 1.5 mm track 500 times, at approximately 1 mm/s. The initial normal load ranged from 5 - 6 N. Load changes as a function of sapphire ball wear, such that the change in load is a measure of wear rate. A new ball was used for each test so that the extent of wear could be determined from the change in the ball's volume. Tests were performed in room air under both dry (25% RH) and humid (50-60% RH) conditions.

In the pin-on-disk tests, the tests were made using a bi-directional pivot arm. The normal force is a dead-load (z-axis applied). The tangential force is measured by an in-plane arm pivot and a load cell. A schematic diagram of the instrument is shown in Figure 4b. The sample rotates under the stylus so that the wear tracks form a circle. In these tests, circle radius varied from 3 - 18 mm. A constant normal load of 2 N was applied during testing. The contact area of the diamond stylus on the sample had previously been worn flat. Test speed ranged from 49 to 125 cm/s. Tests were performed under dry (0% RH) and humid (50-60% RH) conditions.



(a)



(b)

Figure 4: Schematic diagrams of (a) Reciprocating Sliding and (b) Pin on Disk friction testers.

III. RESULTS AND DISCUSSION

The friction of natural diamond on diamond film approaches that of natural diamond on natural diamond ($\mu_{\min} = 0.05$) under some test conditions.

The morphology of faceted diamond films was found to play a more important role than the extent of sp^3 (diamond) bonding in determining tribological behavior, especially in the reciprocating sliding tests. This result indicates that great flexibility in film morphology is attainable without sacrificing tribological characteristics since judicious addition of nondiamond bonded material to the film to achieve maximum smoothness should have little effect on film behavior, at least for applications in which the opposing surface is alumina or sapphire. If the film has so little diamond bonding that it is mechanically soft and/ or exhibits no faceting, a strong correlation between diamond film characteristics and friction was not apparent.

Ambient humidity does not appear to play a role in diamond film tribological behavior.

Substantial variations in film morphology (grain size, grain orientation, surface roughness), diamond bonding content, and growth rate was possible through variation in film deposition conditions.

3.1 Diamond Film Deposition

Group A deposition conditions produced a wide variety of film morphologies and carbon bonding states, allowing a maximum number of film types to be studied within the time allotted. Group B films were predominantly large-grained with purely diamond bonding since the primary goal of this set of experiments was to maximize growth rate while adding as little nondiamond bonded material to the films as possible. Group C conditions produced very smooth films with fine grain size deposited uniformly across the substrate.

The plasma ball was confined to the center of the substrate in groups A and B so that effects of thermal and variation in plasma contact with the substrate could be discerned. Material with cauliflower morphology was deposited outside the plasma contact area while mixed material could be obtained at the perimeter of the contact area. Thus, one sample could be used to study the tribological behavior of a range of diamond bonding and film morphology.

Preliminary tribological test results based on Group A films suggested that smooth films would result in superior tribological behavior. The most direct method for obtaining smooth films is to reduce grain size. Grain growth occurs throughout film deposition, suggesting that thinner films would have finer grain size. In addition, results from perimeter regions (where the plasma is no longer in contact with the substrate) of the films in Groups A and B and some low temperature

experiments indicated that low substrate temperature was the key to smooth diamond films. These hypotheses were confirmed by the results of Group C depositions, all of which were done at lower temperatures and lower power densities than the films in the preceding experiment sets.

A. Group A Films

Group A films produced a wide range of film morphologies and bonding states. Seven different morphologies (illustrated by the micrographs in Figure 5) were generated, as follows:

Table 5: Morphology Ratings standard.

Morphology Rating	Morphology Description	CLA* Range (nm)
1	smooth cauliflower	30 - 40
2	rough cauliflower	50 - 60
3	mixed cauliflower, and (100)/(110) faces	40 - 50
4	dominated by (100)/(110) faces	50 - 70
5	mostly (100)/(110) faces, but other directions also showing growth	60 - 90
6	dominated by (111) faces	70 - 80
7	mostly (111), but with many defects	200 - 300

* CLA stands for *Center Line Average*.

These rankings reflect a qualitative gradation in surface smoothness. It is not possible at this time to accurately determine actual roughness. Roughness is comprised of departures from flatness, grain size, grain orientation, and surface chemistry during testing. Departure from flatness can be determined by CLA values, but the other components are not included in this measure. A film can have a very large CLA due to deep grain boundaries and yet have such large, smooth, nonreactive grains that it behaves as a much smoother film than its CLA predicts. Thus, to determine a morphological rank, the CLA and the appearance of the film are taken into account. In going from rating 1 to rating 7, the films go from cauliflower to (100)/(110) dominated to (111) dominated. Overall, the films are getting rougher in this progression. It has the additional advantage of grouping similar morphologies for ease of observation in plots, as will be shown in the sections on tribological testing.

The films were also rated according to their Raman spectra on a scale of A-F based on sp^3/sp^2 ratio (see Table 6) and, to a lesser extent, on the diamond peak's full width at half maximum. The more closely a film approximates natural, single crystal diamond, the greater its sp^3/sp^2 ratio and

the narrower its FWHM. If a film exhibits two representative types of Raman spectra (e.g., grain boundaries are significant and produce a different spectrum than do the grains), the film is ranked according to the spectrum which shows the least diamond bonding. This ranking is not intended to predict tribological behavior. Raman spectra are shown next to corresponding SEM micrographs. Their Raman rating is also given in Figure 5.

Table 6: Raman Rating standard.

Raman Rating	sp ³ / sp ² Range
A	> 5
B	3 - 5
C	2 - 3
D	1 - 2
E	0.75 - 1
F	< 0.75

Note that films with very strong diamond Raman peaks tend to have faceted grains while, as the amount of nondiamond bonded carbon (Raman peaks at 1340 - 1370 cm⁻¹, and 1550 - 1600 cm⁻¹) increases, the grain edges become more rounded. Thus, to first order, film morphology is an indication of diamond content. However, it is dangerous to draw conclusions of a film's bonding state(s) based solely on its morphology; analysis of Raman data is still the best technique for positive identification of diamond bonding in thin films.

B. Group B Films

Group B films produced Raman spectra that were all in the A-B range, i.e., exhibiting little or no graphitic bonding. All the higher temperature material yielded very large grains, none of which were distinctively (100) or (110) oriented. As a result, these films are very rough. They were not subjected to tribology tests in part because of their high roughness. Typical Group B film morphologies, accompanied by their corresponding Raman spectra, are shown in Figure 6.

Group B deposition conditions did produce the highest film growth rates. Temperature and carbon monoxide concentration in the reactant gas mix were found to be the determining factors for deposition rate. Higher temperatures produced higher growth rates while, given a minimum methane concentration, increasing amounts of carbon monoxide yielded both higher growth rates and better Raman spectra. When no methane was present, however, the films grew very slowly. Carbon monoxide is either less efficient as a diamond precursor or it severely etches the growing film. A comparison between pure methane and pure carbon monoxide Raman spectra is shown in Figure 7.

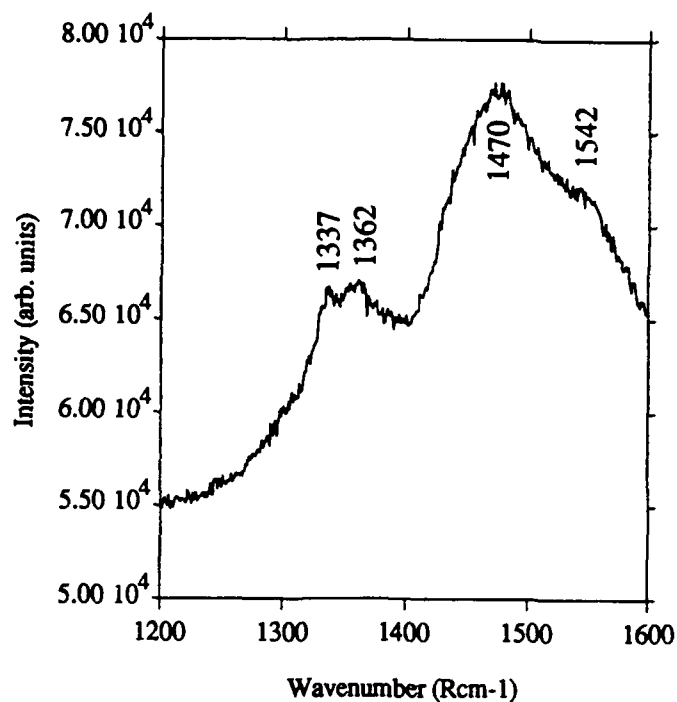


Figure 5a: SEM micrograph (left) and Raman spectrum (right) showing film with morphology rating 1 and Raman rating F.

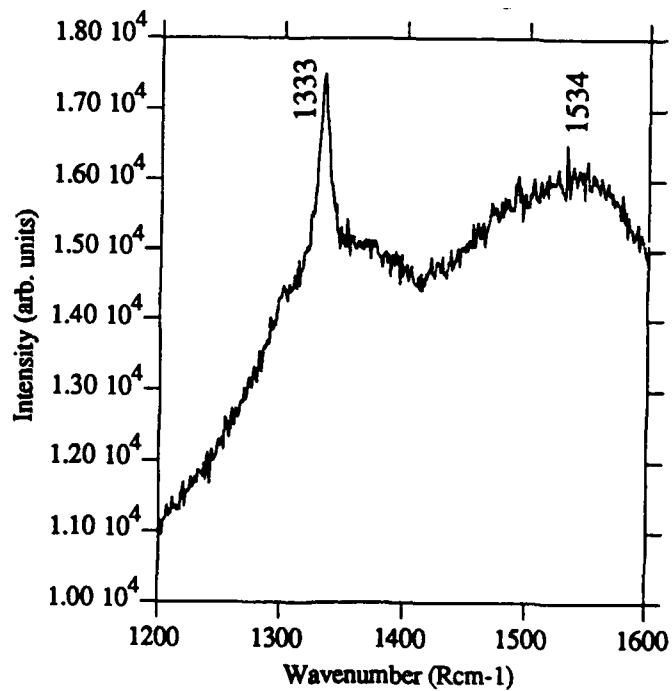
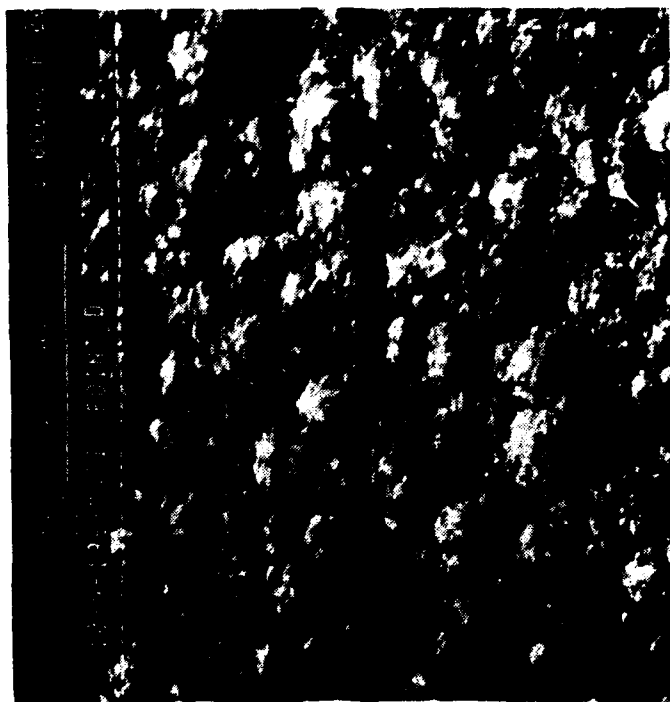


Figure 5b: SEM micrograph (left) and Raman spectrum (right) showing film with morphology rating 2 and Raman rating D.

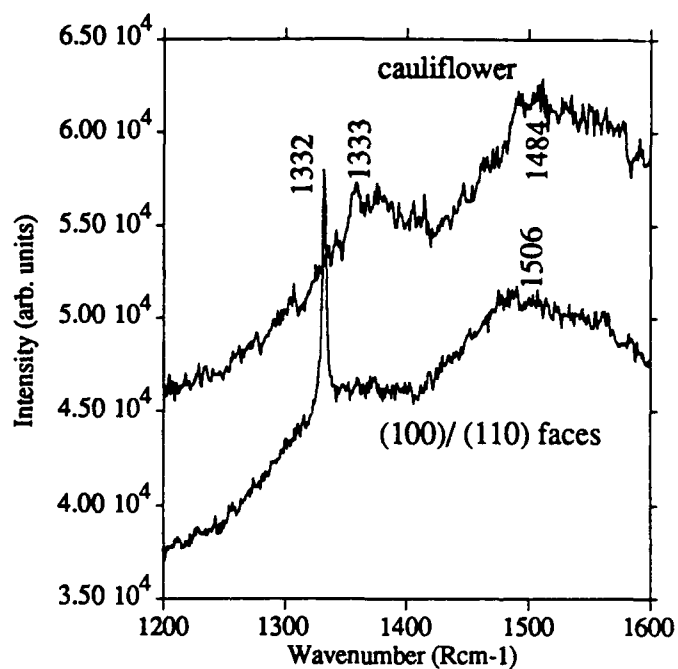
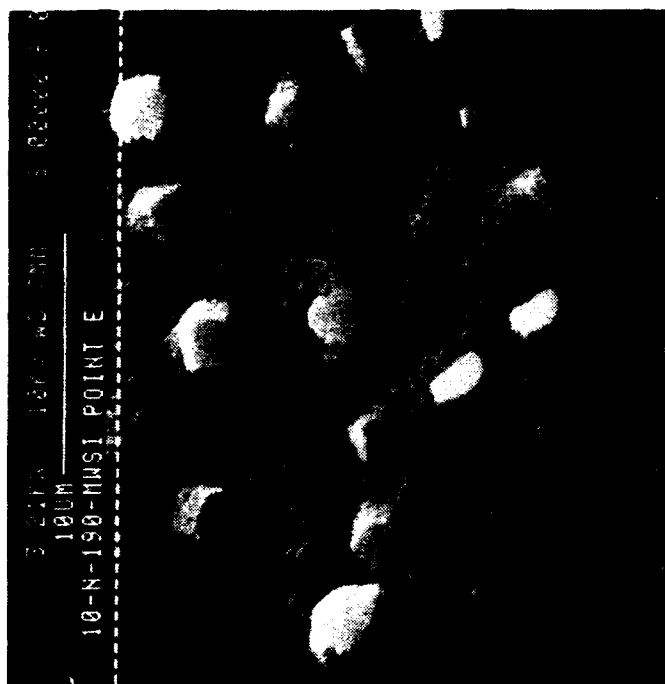


Figure 5c: SEM micrograph (left) and Raman spectra (right) showing film with morphology rating 3 and Raman rating E.

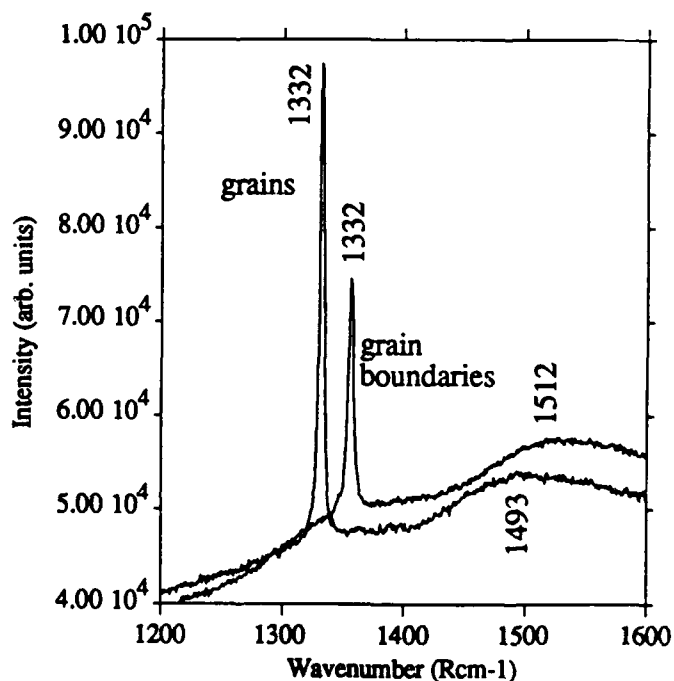


Figure 5d: SEM micrograph (left) and Raman spectra (right) showing film with morphology rating 4 and Raman rating B.

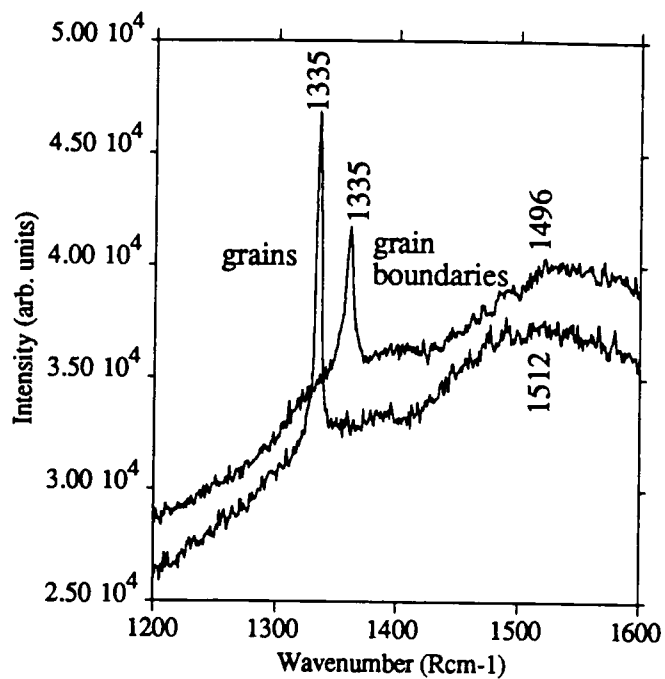
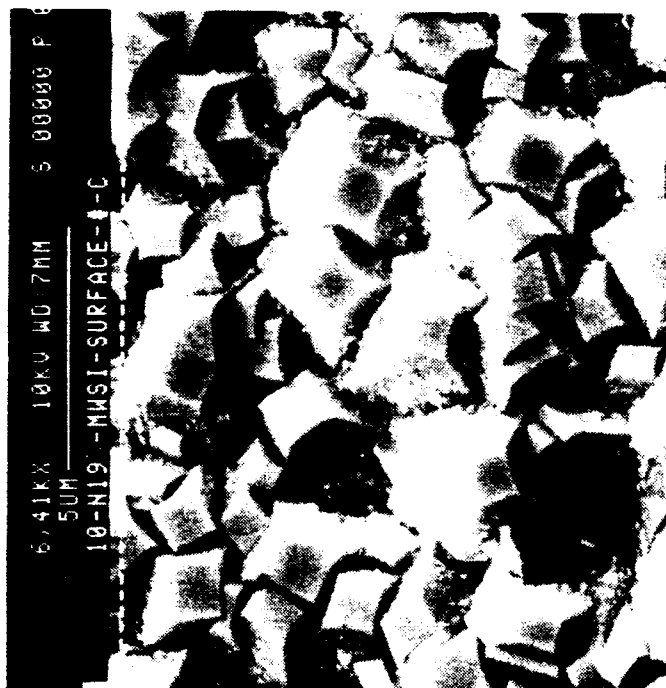


Figure 5e: SEM micrograph (left) and Raman spectra (right) showing film with morphology rating 5 and Raman rating D.

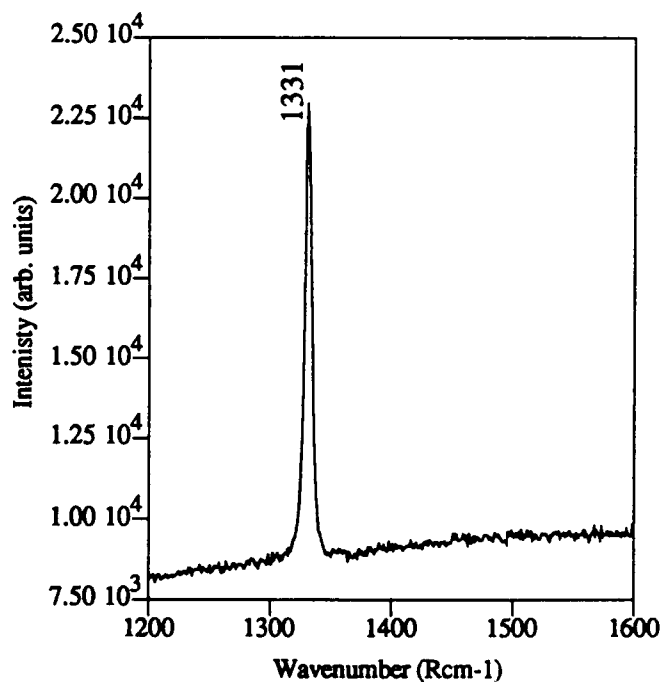


Figure 5f: SEM micrograph (left) and Raman spectrum (right) showing film with morphology rating 6 and Raman rating A.

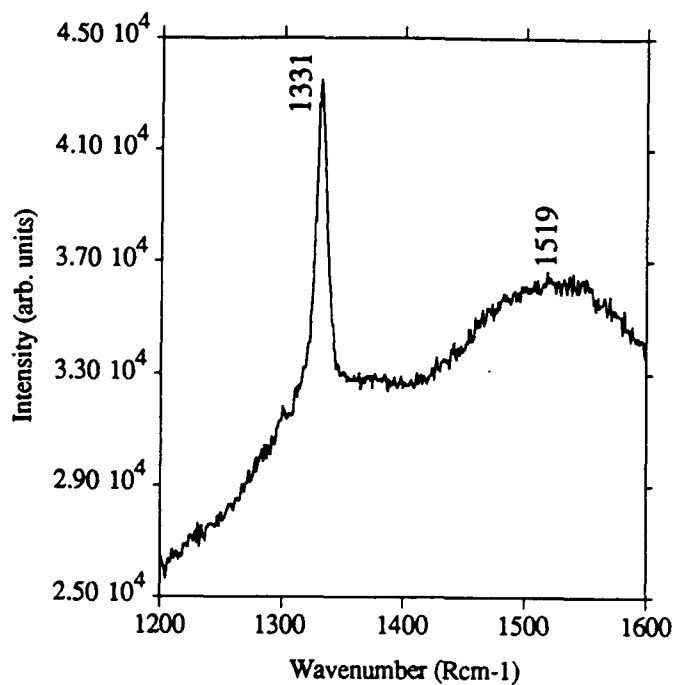


Figure 5g: SEM micrograph (left) and Raman spectrum (right) showing film with morphology rating 7 and Raman rating C.

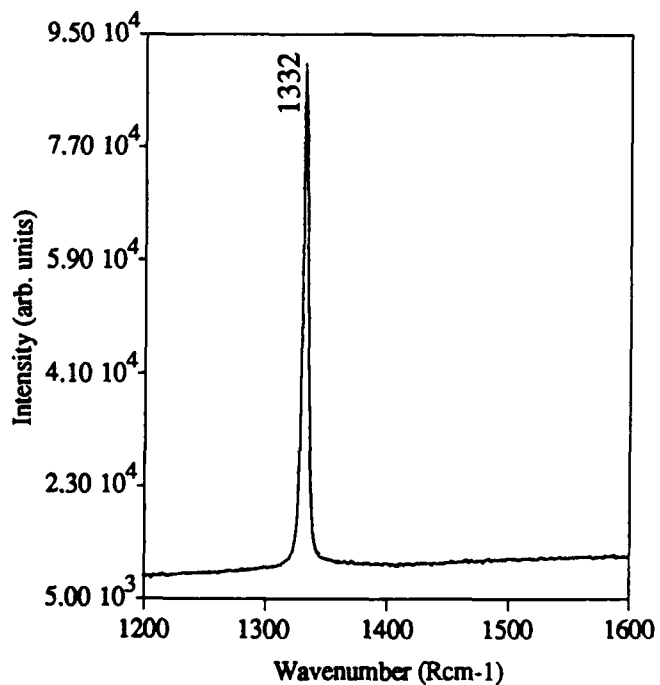
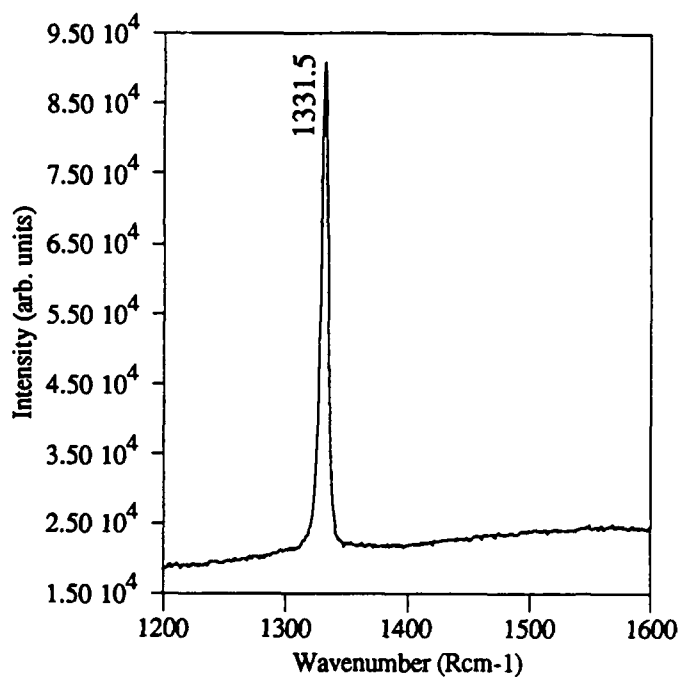
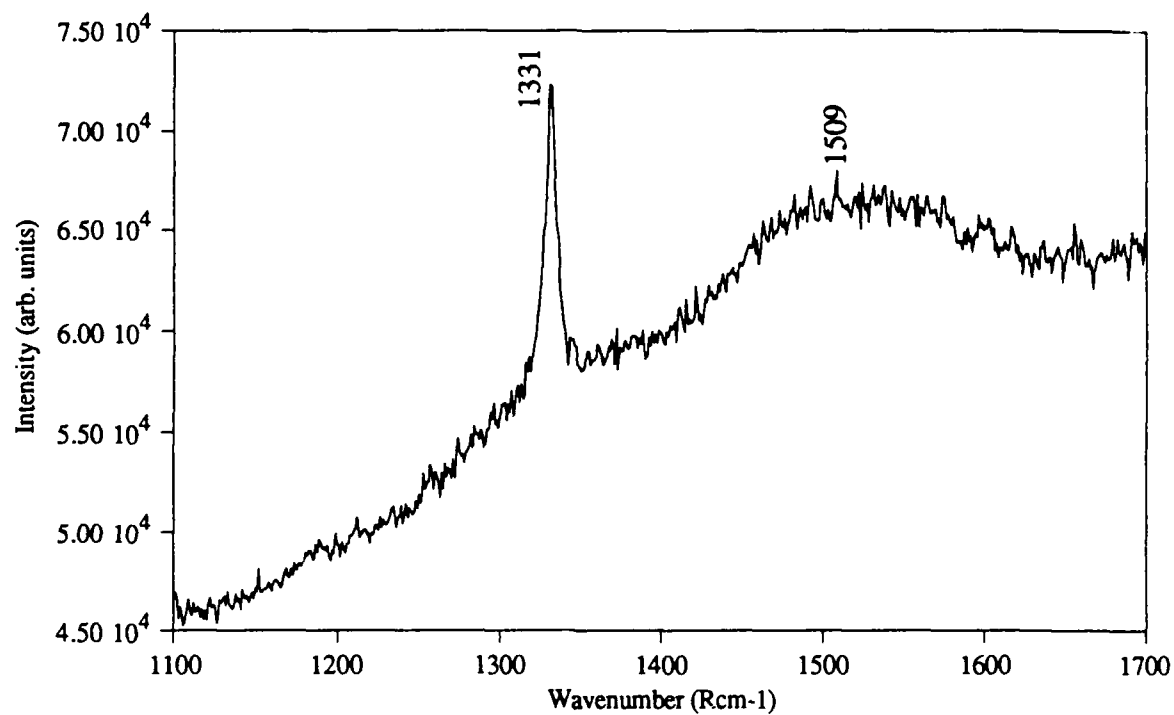
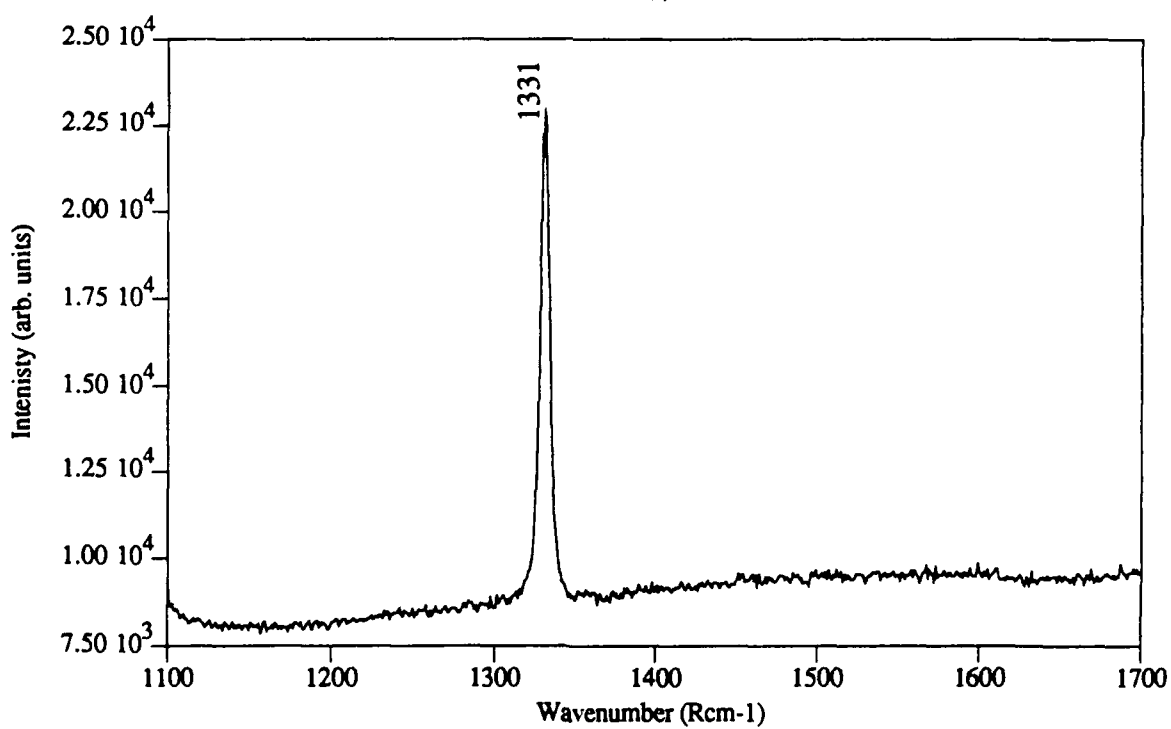


Figure 6: SEM micrographs (left) and Raman spectra (right) from two films typical of Group B deposits. Large grain sizes and high sp^3/sp^2 ratios were common in this Group.



(a)



(b)

Figure 7: Raman spectra from diamond films deposited using (a) only methane or (b) only carbon monoxide as the carbon source. Conditions were otherwise held constant.

C. Group C Films

Film morphologies and corresponding Raman data for the Group C films (fine grained, smooth films) are shown in Figure 8. These films exhibit a narrow range of film morphologies, although the Raman spectra vary dramatically. The relatively small, broad diamond peak from the diamond film deposited by DC plasma excitation is probably due to the destructive effects of electron bombardment of the growth surface during deposition, i.e., the electron bombardment may be responsible for the dendritic growth commonly observed in DC films [1, 13].

All films in this Group showed an increase in surface smoothness over the previous Groups. CLAs for Group A films ranged from 30 to 350 nm while Group B films typically exhibited 250 - 500 nm CLA compared to Group C film CLAs which were all under 25 nm CLA (with the exception of the deposits on silicon carbide, which were still very rough in spite of reduced grain size). Because of time limitations, no tribological analysis of this group of films was performed.

D. Films Deposited on Silicon Carbide

There are two main differences between the silicon carbide and silicon substrates (other than the fact that they are different materials): (1) The silicon carbide substrates are formed from polycrystalline material while the silicon is single crystal and (2) the silicon carbide substrates are in block form, of dimensions 1 x 2 x 4 cm, compared to the 2" wafer form of most of the silicon substrates. The polycrystalline nature of the films tends to encourage growth of large grains in the diamond films, as evidenced by the micrographs in Figure 9, which show deposits on silicon and silicon carbide substrates performed under otherwise identical conditions. While diamond abrasion of the surface did encourage uniform deposition on the silicon carbide substrate, it did little to maintain fine grain size. In addition, the large size and reasonably good thermal conductivity of the silicon carbide substrates (see Table 3) strongly affects substrate temperature. By intentionally decreasing substrate temperature, fine grains were attained even on silicon carbide (Figure 10).

E. *In Situ* Film Planarization

As diamond films increase in thickness, grain growth occurs. Films twice the thickness of those shown in Figure 8 would have significantly larger grains than those shown, and the surface would be that much rougher. For other rough, CVD deposited materials, an *in situ* etch and redeposition cycle is often used to planarize the growing surface. Variations on this technique were attempted here. To this end, several films were exposed to a hydrogen plasma etch. No improvement in surface roughness was seen. In another experiment, a new film was nucleated on a rough diamond film. In spite of the attempt at renucleation, the grain size of the original film dominated and large grains resulted, as shown in Figure 11. This effect is similar to that of polycrystalline silicon carbide shown in Figure 9, where the large grain size of the substrate appears to assist in the growth of large diamond grains. The second film was not different in any

noticeable way from a film that had been grown without interruption. However, higher temperatures, plasma densities, and deposition pressures may improve the etching and redeposition effect by increasing the growth and nucleation rates. Alternatively, lower temperatures, which typically result in fine grain size, may be the key to success in this endeavor. Future work should focus on this practical problem.

Once a reproducible method for planarization has been detailed, thick tribological coatings will become practical. For such a film, a thick layer of rapidly grown, rough film could be completed with a thin, planarizing layer. The composite film could then be expected to exhibit some of diamond's desirable properties, such as high thermal conductivity, even if the top layer contained some nondiamond bonded material.

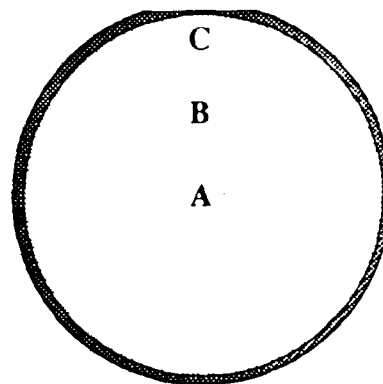
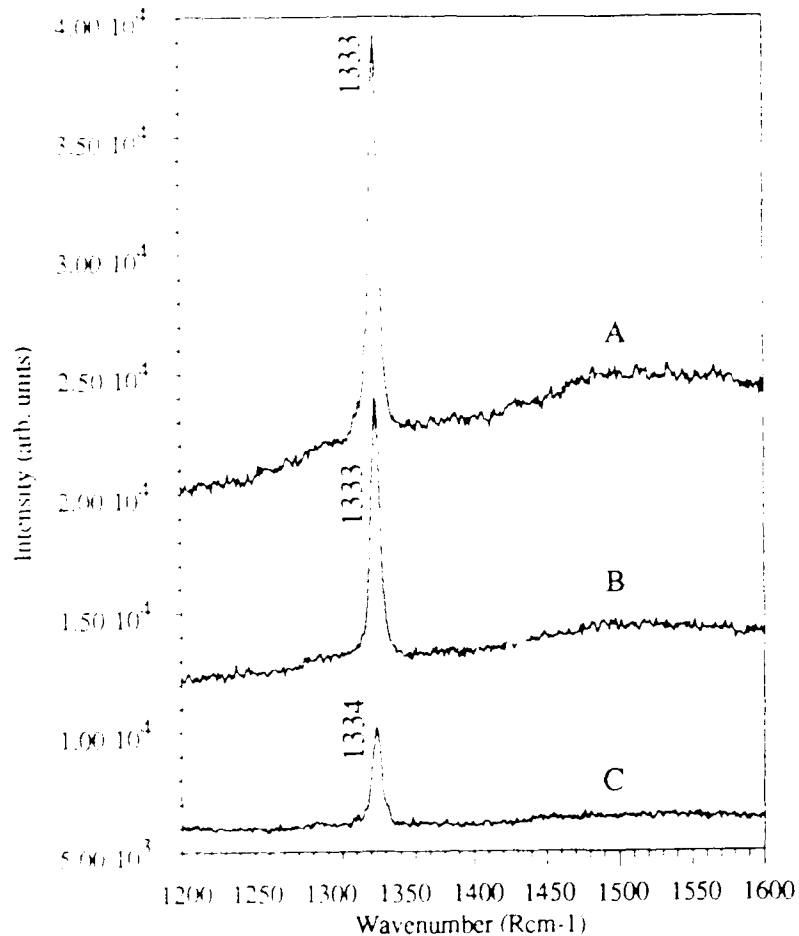
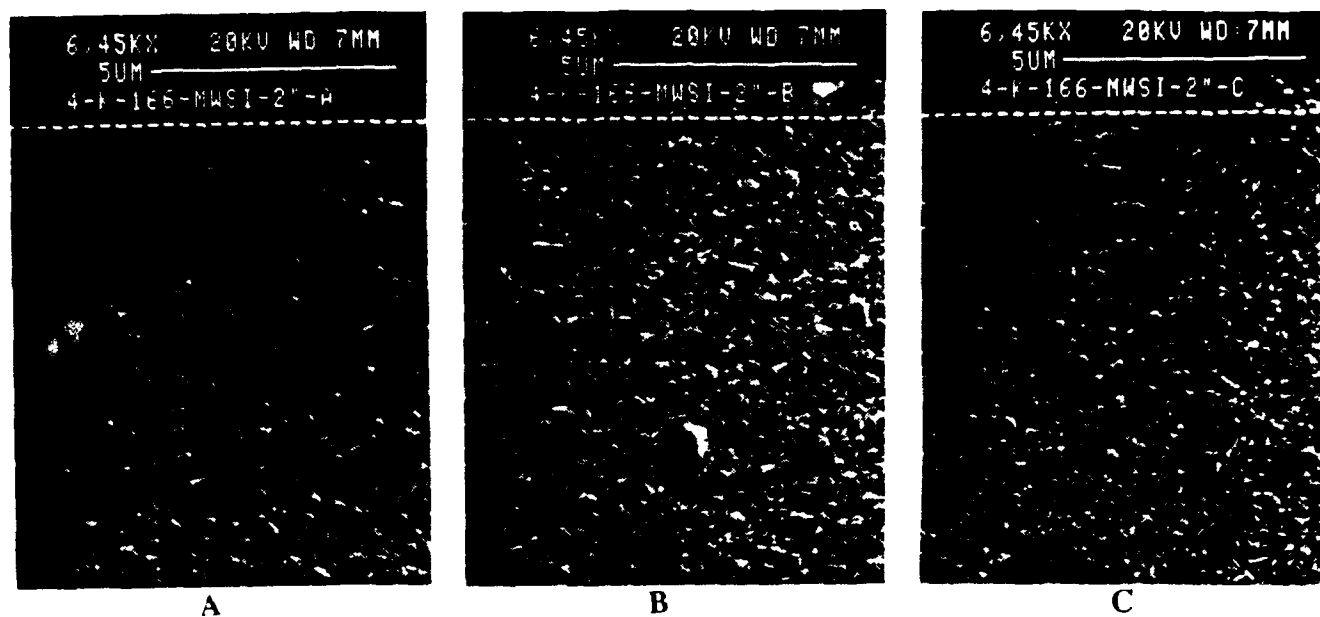
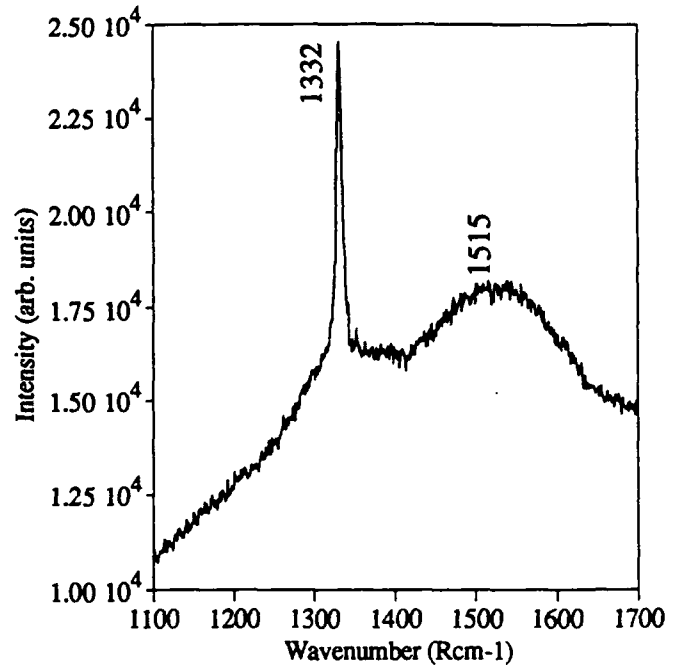
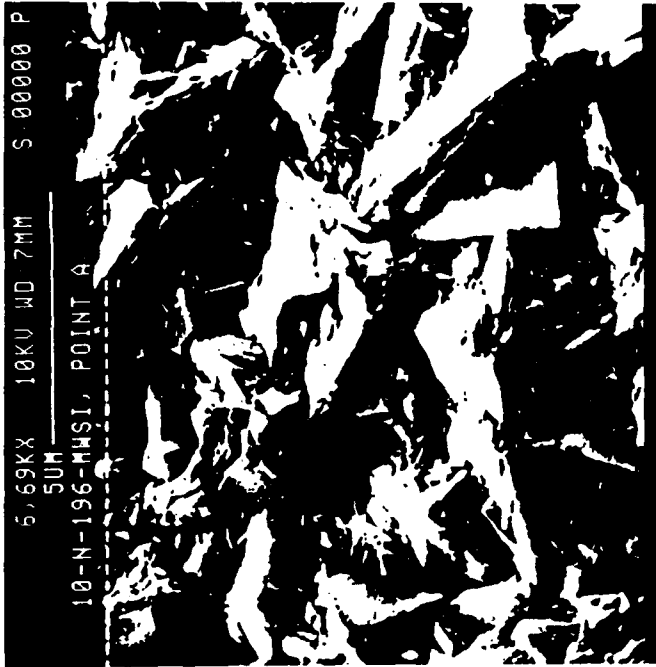
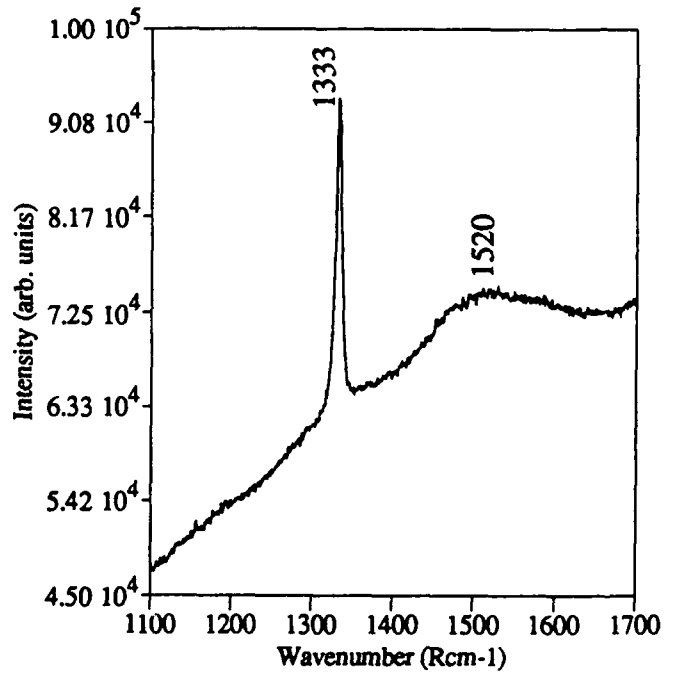
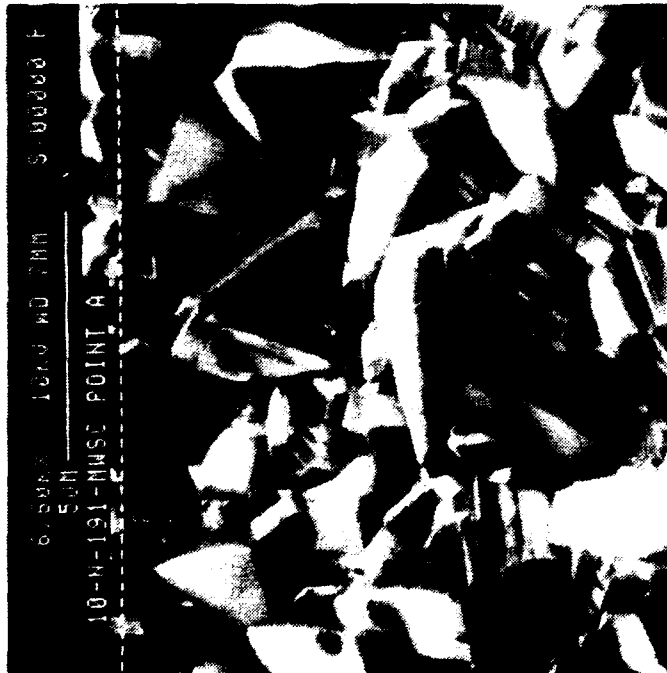


Figure 8: SEM micrographs (top) and Raman spectra (left) showing film bonding and morphological uniformity across a two inch silicon substrate. The main difference between the Raman spectra is in signal intensity, which is a function primarily of film thickness.



(a)



(b)

Figure 9: SEM micrographs (left) and Raman spectra (right) showing effect of substrate on film morphology and bonding. (a) Silicon substrate. (b) Silicon carbide substrate.

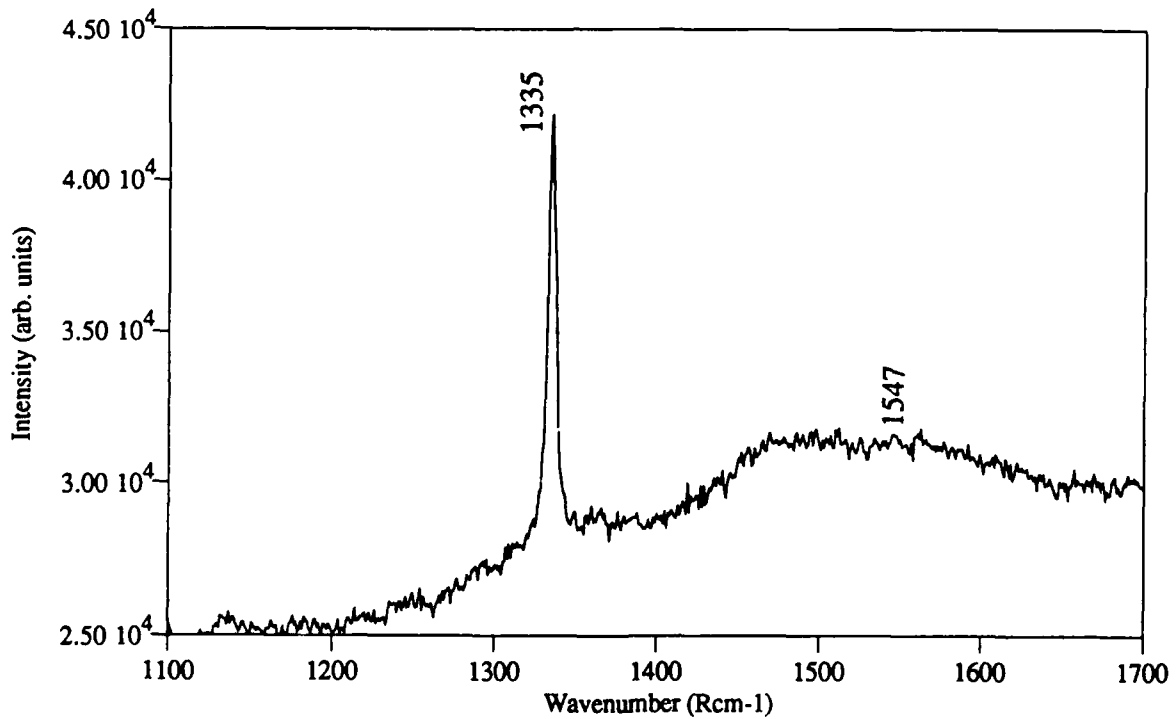
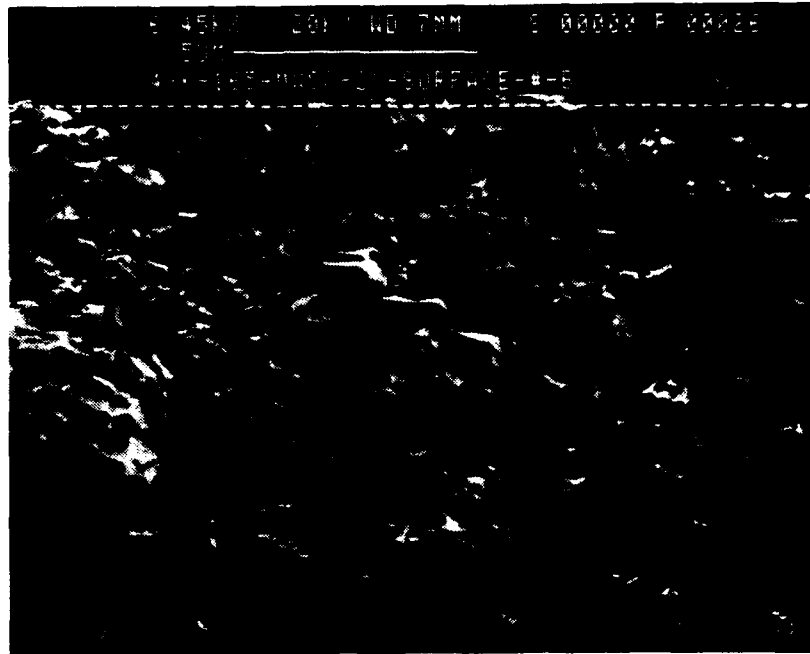
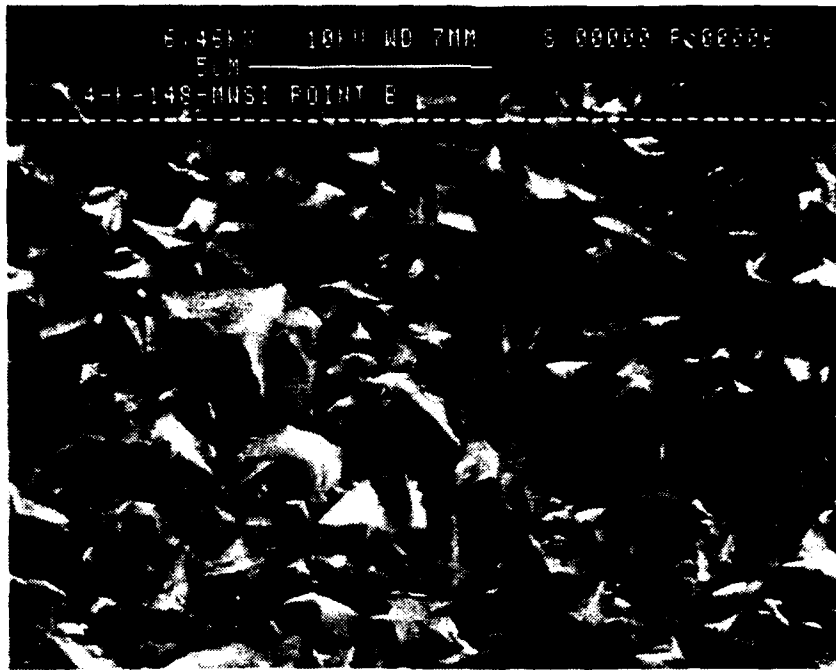


Figure 10: SEM micrograph (top) and Raman spectrum (bottom) for low temperature deposit on silicon carbide. Note that grain size is smaller but the Raman spectrum is quite similar to the higher temperature deposition shown in Figure 9b.



(a)



(b)

Figure 11: SEM micrographs (a) before and (b) after hydrogen etch and redeposition cycle. Note that grain size and apparent roughness were not reduced by the process.

3.2 Tribology Test Results

The tribological properties friction and wear were studied using pin on disk (natural diamond on diamond film) and reciprocating sliding (sapphire on diamond film) tests. In the following discussion, coefficient of friction is abbreviated as μ ; subscripts i, f, and min refer to initial, final, and minimum coefficients of friction.

A. Tribology Results: Reciprocating Sliding Tests

A summary of the results of reciprocating sliding tests follows:

- Sapphire stylus wear increases with increasing initial film roughness.
- Film morphology appears to be the strongest determinant of μ_i .
- Films dominated by (111) planes have higher μ_i than those dominated by (100) and (110) planes.
- In the range studied, humidity had no significant effect on μ_i .

Reciprocating sliding tests were performed with a sapphire stylus. Alumina is a widely used material in tribological applications, so the friction and wear behavior of diamond films against sapphire is of general interest. In addition, similar materials attempt to chemically bond to each other during tribological testing, enhancing adhesion, so that diamond on diamond tests can be difficult to interpret. Employing a sapphire stylus prevents this problem.

Sapphire is not as hard as natural diamond so extensive wear can be expected when rough films are tested. The process of wear leads to transfer of alumina from the ball to the film (or, in the case of highly nondiamond (relatively soft) films, transfer from the film to the ball). As a result, the surfaces being tested soon become sapphire on alumina or carbon on carbon, complicating analysis.

Wear was measured in all reciprocating sliding tests *via* changes in the normal load on the sapphire ball. As described in §2, the reciprocating friction tester applies normal force to the film with a cantilever. Since the deflection of the arm is small, the force is proportional to the deflection. If the ball wears during the test, the arm gradually relaxes and the load drops. For this reason, the difference between final and initial loads can be taken as proportional to the depth of wear of the ball. Large amounts of debris between the stylus and the sample will negate this relationship. Comparison between actual and predicted wear flat size yields good agreement, indicating that the relationship between load and wear depth is valid. The ratio of final to initial normal force is plotted against film roughness in Figure 12. This graph illustrates the strong dependence of wear on initial film roughness.

Initial coefficient of friction is plotted as a function of initial surface roughness in Figure 13. This data is complicated by the effects of stylus wear. Initial coefficient of friction, as presented on the graph, is the calculated mean of the values from the first two test passes. As a result, a rougher

film may have an artificially low μ_i because of the following mechanism: A very rough film may have very high friction on the first pass due to surface roughness. Because it is rough, substantial wear of the stylus occurs, followed by significant transfer to the film surface. Sample friction on the second pass may then be substantially lower, since it will be representative of sapphire on alumina. The mean would thereby be substantially lowered from its true value. Nonetheless, trends based on film morphology are evident, as discussed in the next paragraph, indicating a need for further testing.

The cauliflower films exhibit too much scatter to be useful in analyzing trends and have been omitted from the graph in Figure 13. There does, however, appear to be a correlation between μ_i and the surface morphology of the faceted films. The films exhibiting predominantly (111) planes have a markedly higher initial coefficient of friction than those with (100) and (110) facets. In addition, μ_i of the former material increases with increasing surface roughness. There are insufficient data to establish a similar relationship for the (100)/(110) material. It is evident from the graph that film morphology (rather than surface roughness alone) plays an important role in this behavior. The diamond bonding content of the films represented in Figure 13 show no correlation to μ_i .

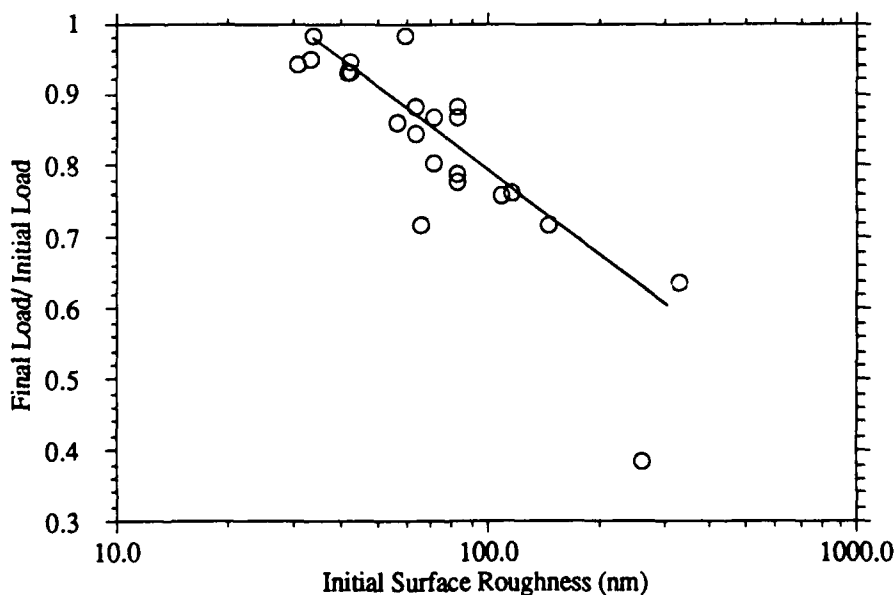


Figure 12: Ratio of final stylus load to initial stylus load as a function of initial surface roughness.

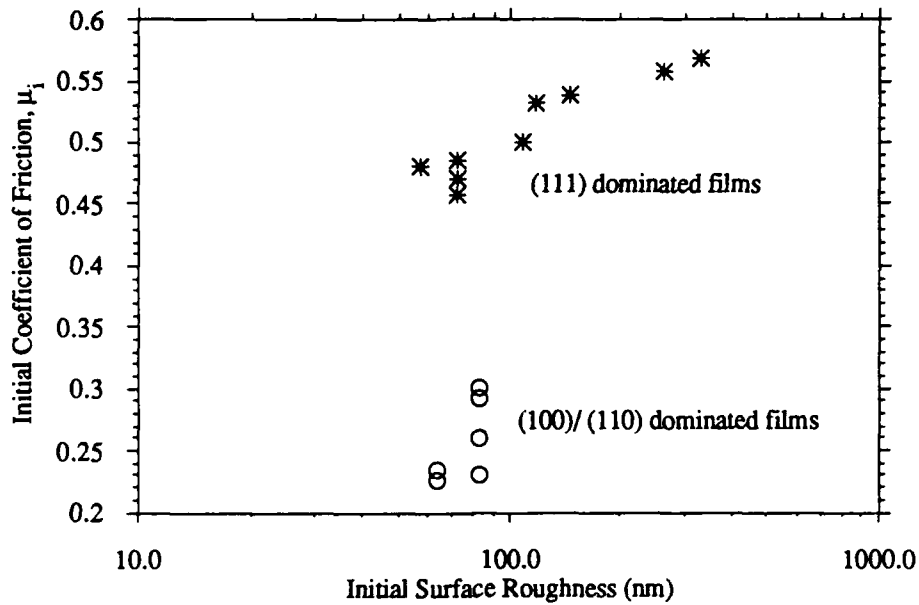


Figure 13: Initial coefficient of friction as a function of initial surface roughness and film morphology. (100)/(110) films exhibit significantly lower μ_i than do (111) films.

The importance of film morphology in determining μ_i is most strongly demonstrated by the next plot, Figure 14. The morphology ranking system was discussed in §3.1A and is summarized in the Table 5, which is reprinted below. The cauliflower films (morphology ratings 1-3) have widely dispersed μ_i , while the films with faceted grains show a marked increase in μ_i as the films become rougher and dominated by (111) planes.

Morphology Rank	Morphology Description	CLA* Range (nm)
1	smooth cauliflower	30 - 40
2	rough cauliflower	50 - 60
3	mixed cauliflower, and (100)/(110) faces	40 - 50
4	dominated by (100)/(110) faces	50 - 70
5	mostly (100)/(110) faces, but other directions also showing growth	60 - 90
6	dominated by (111) faces	70 - 80
7	mostly (111), but with many defects	200 - 300

* CLA stands for Center Line Average.

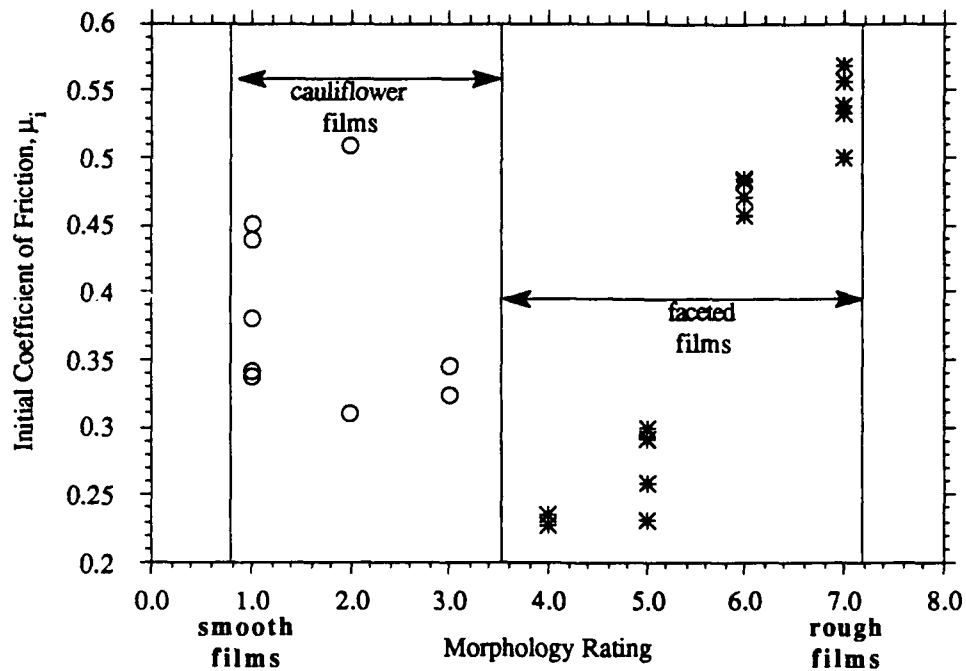


Figure 14: Initial coefficient of friction as a function of film surface morphology. Cauliflower data is scattered, but faceted films show increased μ_i for (111) dominated films.

Humidity, as illustrated by the graph in Figure 15, has no obvious effect on μ_i . Future work should include measurements at higher humidity to insure that no trend is being obscured by the narrower humidity limits studied here. Dry conditions would probably be of limited interest because sapphire exhibits greater adhesion in dry air due to changes in its surface chemistry. The adhesion can reach a level high enough to interfere with proper operation of the tester.

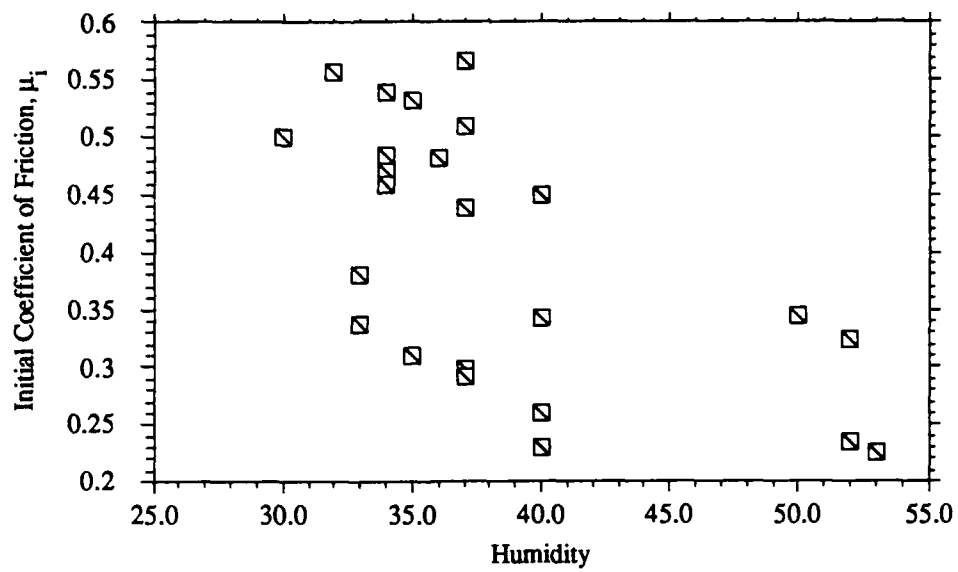


Figure 15: Initial coefficient of friction as a function of humidity.

B. Tribology Results: Pin on Disk

Pin-on-disk (Pod) tests employ a diamond stylus and produce circular wear tracks. In general, tests in which a material is rubbed against another piece of the same material are complicated by strong adhesive tendencies between the two surfaces. Natural diamond on natural diamond, however, shows relatively little adhesion if the test is performed in air. In air, the diamond surface is always terminated with non-carbon atoms which form a protective layer, as discussed in §1.2. Diamond films are also terminated in non-carbon atoms, usually hydrogen, so adhesion due to formation of diamond bonds between the opposing surfaces only becomes significant if the surface layer is worn away and other atoms are not available to tie up the dangling bonds (e.g., *in vacuo*).

Wear of both stylus and film were observed during testing. Friction measurements may be affected by build up of debris. In the reciprocating sliding tests, debris tends to build up at either end of the linear wear track. In Pod tests, since the wear track is circular, wear debris can be present in all parts of the track. Diamond debris can affect tribological behavior by behaving like roller bearings between film and stylus or by lodging between asperities and thereby changing film roughness.

Pod results can be summarized as follows:

- Minimum coefficient of friction was found to approximately 0.05 for all films.
- Initial friction is somewhat dependent on initial film roughness, but more work is needed.
- Initial friction is also a function of film diamond content.
- Humidity has no strong effect on film tribological behavior.

Figure 16a shows initial, minimum, and final coefficients of friction from all tests as a function of surface roughness. The strongest trend exhibited by these data was that, in almost every test, the minimum coefficient of friction approached that of natural diamond, 0.05. The μ_i data is replotted in Figure 16b on an expanded scale to illustrate this trend. Final friction tended to be somewhat higher than the minimum. This increase is probably due to a combination of processes: Wear of the stylus leads to its roughening and the production of debris, which in turn causes polishing of the film in the wear track. If the polishing is such that the contaminant surface layer is worn through, adhesion between the surfaces can increase. Other mechanisms may be playing a role.

Initial coefficient of friction is plotted against initial surface roughness in Figure 17a (cauliflower film data is omitted because of its wide scatter). Unlike the reciprocating sliding results, initial friction appears to be more dependent on film diamond content and surface roughness, and less so on the crystal faces apparent on the film surface. In the reciprocating sliding tests, all (111) dominated films exhibited about the same μ_i and all (100)/(110) films were

similarly clustered about a different μ_i . In the pin on disk tests, it is surface roughness (Figure 17a) and/ or film diamond content (Figure 17b) that help determine μ_i . The data for faceted films in Figure 17b indicate a trend of increasing μ_i for increasing nondiamond bonding in the films.

Humidity does not appear to play an important role in determining film tribological behavior since no trends were observed for initial, minimum, or final friction as a function of humidity.

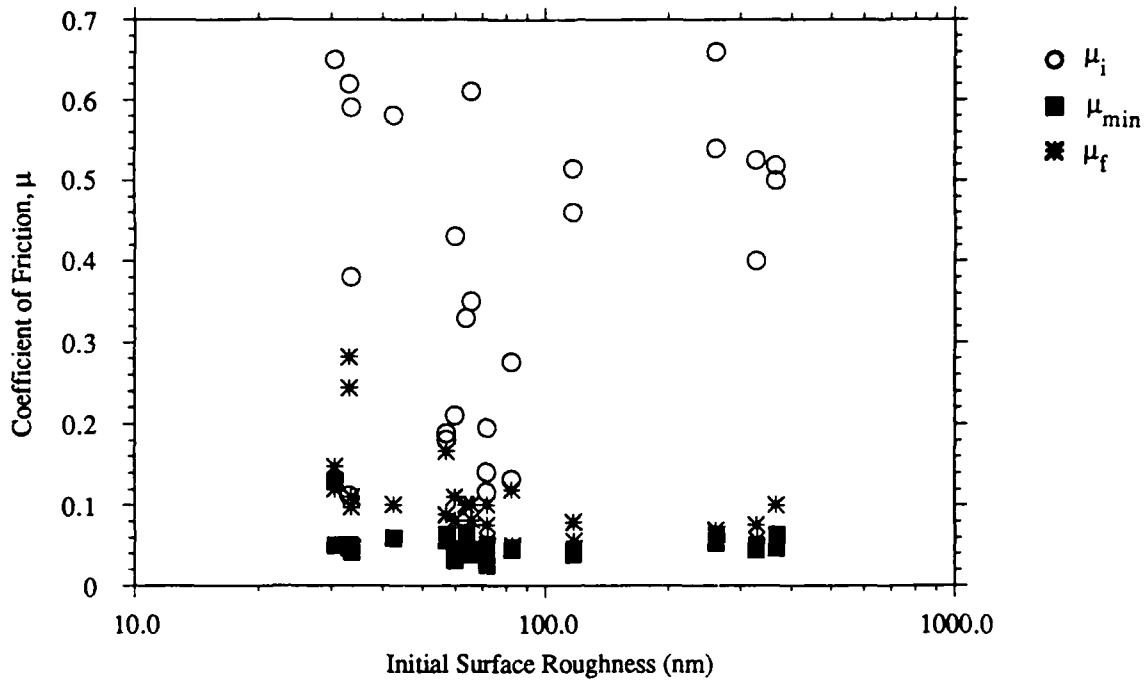


Figure 16a: Coefficient of friction as a function of initial surface roughness for initial, minimum, and final measurements.

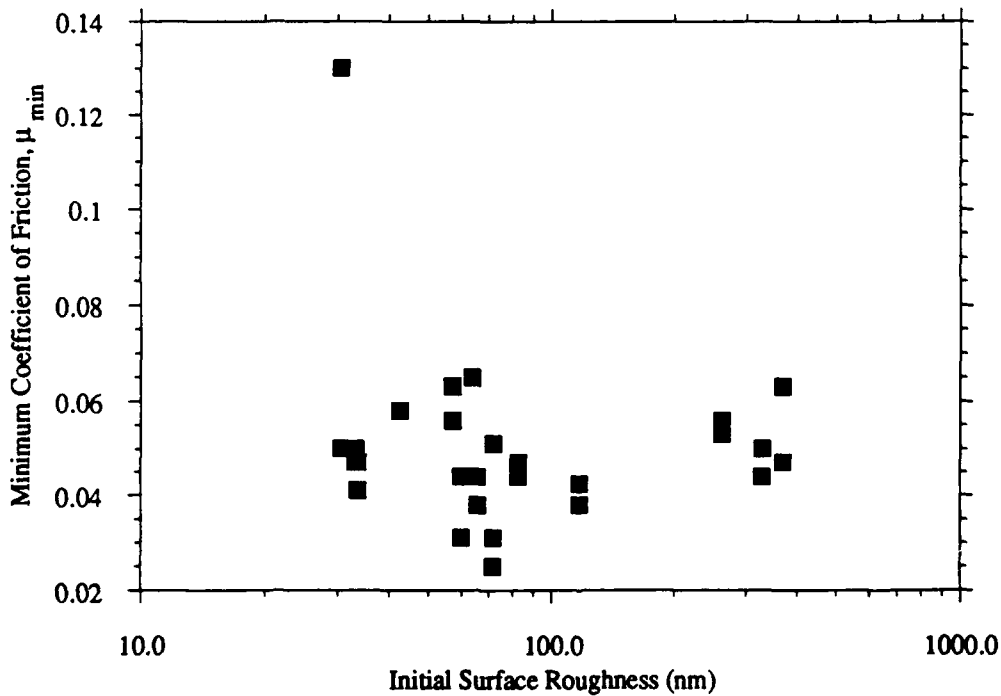


Figure 16b: Minimum coefficient of friction as a function of initial surface roughness.

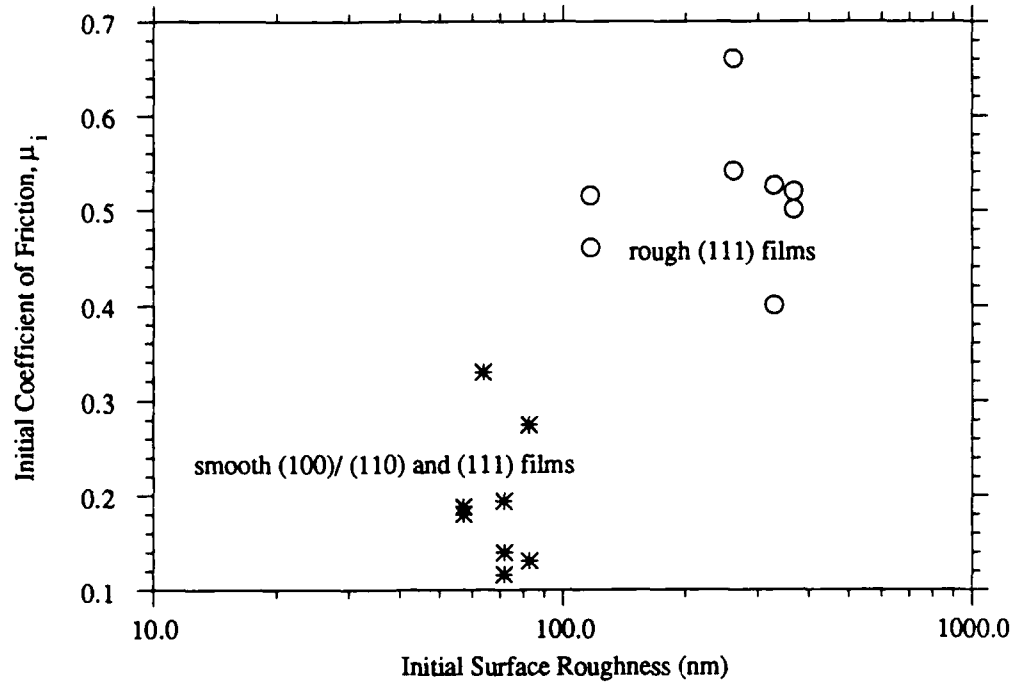


Figure 17a: Initial coefficient of friction as a function of initial surface roughness showing morphology dependence of μ_i .

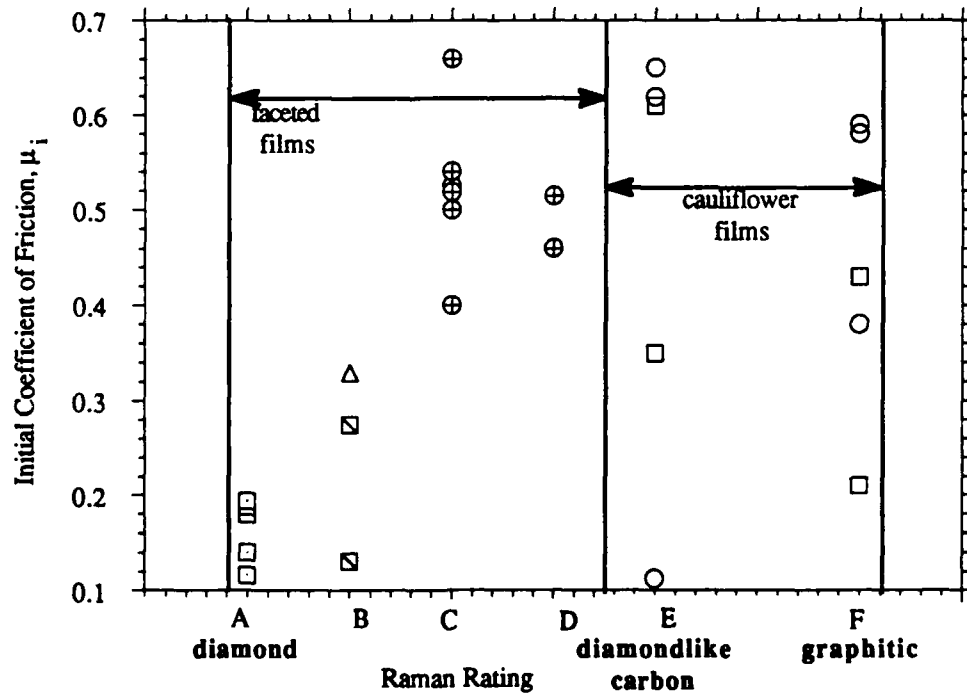


Figure 17b: Initial coefficient of friction as a function of film diamond bonding content. Increasing nondiamond content appears to increase initial coefficient of friction for non-cauliflower morphologies.

C. Summary of Tribology Test Results

In the reciprocating sliding tests, an initially smooth sapphire ball slides on a comparatively rough surface. The ball experiences severe wear due to the abrasive action of the diamond film surface. Gradually, wear debris is transferred to the film so that, eventually, the sapphire ball is sliding on wear debris instead of diamond. Once a complete layer has formed, the sapphire ball is sliding on a material very similar to sapphire. Friction is quite high due to chemical bonding between the two, similar materials. Humidity in the air can react with the surface of the transferred material. If the coating becomes hydrated, the friction will drop again since then the sapphire ball will be sliding on a material that is significantly different from sapphire.

Friction between diamond films and sapphire is therefore expected to be a function of initial film roughness. Initial friction and ball wear have both been shown to exhibit this dependence. Friction also appears to be a function of other film morphology factors (e.g., grain size and orientation), although additional work is needed to verify this trend. It is possible that the observed effects are due to different surface chemistry associated with different crystal faces, rather than mechanical effects. Surface chemistry affects friction by altering the adhesion component of friction or by changing the transfer rate.

Some of the diamondlike carbon films showed evidence of transfer from the film to the stylus. In this case, the test surfaces would become carbon film on carbon film rather than sapphire on sapphire. Since these carbon films contain a variety of bonding types and probably a good deal of hydrogen, it is not surprising that the resulting tribological data shows considerable scatter.

The diamond-on-diamond pin on disk tests show that friction behavior of diamond films can approach that of natural diamond. All films, regardless of diamond bonding content, film morphology, and ambient humidity reached $\mu_{\min} = 0.05 \pm 0.03$ at some point in the test. Final friction tended to be higher than the minimum, although not nearly as high as initial friction. A likely explanation for this is the presence of wear debris, although more study is necessary to determine its role.

Unlike the case of the reciprocating sliding tests, initial friction appeared to be a function of initial surface roughness and of diamond bonding content. Grain orientation did not appear to play a role.

Wear of both stylus and film occurred during testing, probably because of the roughness of the films. Humidity had no apparent effect on tribological behavior.

IV. FUTURE WORK

Future research into the tribological behavior of diamond films should include the following general directions: (1) Further investigation of smooth, fine-grained films, (2) in-depth study of the role of wear debris in friction, and (3) analysis of surface and surface modification effects.

While smooth films have already been deposited, methods for optimizing their growth, especially in terms of growth rate, should be explored. Possible avenues include more complete work on *in situ* planarization through etch and regrowth, development of films with truly preferentially oriented grains, and compound structures in which the lower layer is thick, high quality diamond and the top layer has the smoothness required for low friction. In addition to smooth films, more work should be done on varied morphology films to confirm or refute the trends documented in the previous section. Chemical modification of the film surface may be performed to obtain C_3N_4 , a compound that has recently been found to be capable of scratching diamond [14]. Deconvolution of the effects of various aspects of film morphology on friction may also be possible after sufficient testing.

The issue of wear debris can also be attacked in several different ways. Since the amount of debris is a function of the roughness of the film surface, part of the research into wear debris should include further study of films with a wide range of roughnesses. The work already performed indicates that roughness is a factor in determining friction, but these results should be confirmed and expanded. Improved correlation between wear rate calculated from changes in normal load for the reciprocating sliding wear tests and actual wear rate can be achieved by stepping the tests. In a stepped test, each full test of, for instance, 500 cycles would be made up of a series of runs, each of shorter duration than 500 cycles. After each abbreviated run, analysis of the stylus and the film would be performed. Transfer debris can also be analyzed in terms of thickness and chemical composition through Auger spectroscopy. Similar tests can be performed with the pin on disk tester.

Finally, the film surfaces should be studied in greater detail so that chemical effects of friction on diamond may be better understood. Reflection infrared spectroscopy and other surface techniques would be of use here. Surface modifications, such as the application of water or lubricants should also be tested since they may greatly affect friction and wear behavior.

V. CONCLUSIONS

Diamond films have exhibited tribological behavior approaching that of natural diamond in diamond on diamond film tests.

For sapphire on diamond film tests, diamond film morphology is the primary determinant of the film's tribological behavior. Film morphology refers to the combination of surface roughness, grain size, grain orientation, and surface chemistry. Surface roughness and grain orientation appear to be the most important of these factors, although more work must be done to deconvolute this information. Rough films dominated by (111) oriented grains tend to have much higher coefficients of friction than do (100) and/ or (110) dominated films. Diamond bonding content had no strong effect on tribological behavior.

In natural diamond on diamond film tests, friction appears to be determined primarily by surface roughness and extent of diamond bonding content. Smoother films with high diamond content exhibit lower friction than do low diamond content films, smooth or rough. Grain orientation does not appear to play a part in determining friction under these conditions.

Small grain sizes yield the smoothest films. These can readily be produced through different plasma excitation techniques and decreased substrate temperature. However, growth rates for such films are relatively low.

Humidity does not appear to play a strong role in diamond film friction and wear.

VI. IMPLICATIONS OF PHASE I RESULTS FOR PHASE II RESEARCH

The goal of Phase II activities will be to extend the work discussed in this report to include erosion-resistant coatings. The deposition work which led to fine-grained, hard coatings will be expanded so that these properties, which are desirable both for tribological and for optical coatings, can be applied to applications encompassing hard coatings from ball bearings through protective coatings for IR optics. In addition to the erosion resistance of the films, additional work on general wear resistance must be performed.

VII. REFERENCES

1. L.S.Plano, J.M.Pinneo, and K.V.Ravi, "Oxidation Resistant Coatings for High Temperature IHPTET Applications;" Final Report for Air Force SBIR Contract No. F33615-88-C-2852; 7 April 1989.
2. J.E.Field, ed.; The Properties of Diamond; Academic Press, NY; 1979.
3. B.B.Pate, M. Oshima, J.A. Silberman, G. Rossi, I. Lindau, and W.E. Spicer; *Journal of Vacuum Science and Technology*, **A2** (2), pp. 957-960; May 1984.
4. S.Matsumoto, Y.Sato, M.Tsutsumi, and N.Setaka; *Journal of Materials Science*, **17**, pp. 3106-3112; 1982.
5. R.C.DeVries; *Annual Review of Materials Science*, **17**, pp. 161-187; 1987.
6. B.V.Deryagin, D.V.Fedoseev, V.P.Varnin, A.E.Gorodetskii, A.P.Zakharov, and I.G.Teremetskaya; *Soviet Physics-JETP*, **42** (4), pp. 639-640; 1976.
7. N.Fujimori, T.Imai, and A.Do; *Vacuum*; **36**, 1-3, pp. 99-102; 1986.
8. S.Yugo, T.Kimura, H.Kanai, and Y.Adachi; *University of Electro-Communications*; 1-5-1 Chofugaoka, Chofu-shi, Tokyo 182, Japan; personal communication.
9. S.A.Solin and A.K.Ramdass; *Physical Review B*, p. 1687; 1970.
10. L.S.Plano and F.Adar; *SPIE Proceedings*, 822-09, *International Conference on Raman and Luminescence Spectroscopy in Technology*, San Diego, CA; 17-19 August 1987.
11. F.Tuinstra and J.L.Koenig; *Journal of Chemical Physics*, **53**, pp. 1126; 1970.
12. N.Wada and S.A.Solin; *Physica*, **105B**, pp. 353-356; 1981.
13. Y.H.Lee, G.H.Ma, K.J.Bachmann, and J.T.Glass; *Applied Physics Letters*, **56** (7), pp. 620 - 622; 12 February 1990.
14. M. Yoder; presented at the *Electronic Materials Symposium*, Santa Clara, CA; 26 March 1990.

VIII. APPENDICES

Raw data for Reciprocating Sliding and Pin on Disk tests are presented on the following two pages.

Reciprocating Sliding Data

Name	Raman Rating	Morph	Appearance	Morph Rating	Init μ	Max μ	Final μ	Init N	Final N	CLA	Final N/ Init N	Humidity
4190A	B	(100)	clean	1	0.22634	0.26799	0.1494	605.1	510.24	640	0.8432	53
4190B	B	(100)	clean	1	0.23428	0.2741	0.08899	597.55	527.62	640	0.883	52
4190C	E	(100)	in cf	3	0.32457	0.52464	0.34125	563.22	523.3	426	0.9291	52
4190D	E	(100)	in cf	3	0.34521	0.57519	0.41402	593.23	560.58	426	0.945	50
41921	C	(100)	small faces	2	0.23045	0.47096	0.06798	540.23	476.86	828	0.8827	40
41922	C	(100)	small faces	2	0.25893	0.42787	0.07808	506.24	438.55	828	0.8663	40
41923	D	(100)	small faces	2	0.2998	0.50664	0.21522	508.92	395.9	828	0.7779	37
41924	D	(100)	small faces	2	0.29125	0.49537	0.19978	520.48	411.34	828	0.7903	37
41925	F	cf	lumpy	4	0.33787	0.6119	0.56164	504.99	470.29	416	0.9313	33
41926	F	cf	lumpy	4	0.38039	0.51464	0.37497	493.13	458.37	416	0.9295	33
41931	C	(111)	random, def	6	0.53909	0.59341	0.0674	478.57	343.29	1467	0.7173	34
41932	D	(111)	random, def	6	0.53217	0.57953	0.07551	502.3	382.72	1169	0.7619	35
41933	F	cf	smoo ther	5	0.30952	0.51686	0.47861	567.63	556.72	601	0.9808	35
4193A	D	(111)	random, def	6	0.49925	0.50422	0.27992	535.57	406.73	1091	0.7594	30
41941	A	(111)	clean	7	0.4712	0.47492	0.36631	496.5	431.14	720	0.8684	34
41942	A	(111)	clean	7	0.4579	0.45792	0.3329	564.32	453.77	720	0.8041	34
41943	A	(111)	clean	7	0.48488	0.4873	0.17422	469.9	372.9	720	0.7936	34
41944	A	(111)	clean	7	0.48183	0.54646	0.08229	512.59	440.06	603	0.8585	36
41951	E	cf	uniform	5	0.45017	0.52484	0.48758	600.92	585.59	307	0.9745	40
41952	F	cf	smoother	5	0.3419	0.41076	0.22516	608.05	597.41	336	0.9825	40
41961	C	(111)	random, def	6	0.55724	0.60216	0.11921	518.07	199.24	2619	0.3846	32
41962	D	cf	lumpy	4	0.50962	0.56267	0.3234	460.51	331.54	658	0.7199	37
41971	C	(111)	random, def	6	0.56771	0.59627	0.06346	527.49	335.8	3289	0.6366	37
41972	D	cf	lumpy	4	0.43915	0.53675	0.4982	548.2	519.86	332	0.9483	37

Pin on Disk Data

Name	Region	Raman Rating	Morph Rating	CLA	μ id	μ mind	μ fd	μ ih	μ minh	μ fh
190	A	B	1	640				0.33	0.065	0.1
190	A	B	1	640						
192	A&B	B	2	828	0.275	0.044	0.119	0.131	0.047	0.05
192	A&B&C	C	2	828						
192	A&B&C	C	2	828						
192	A&B	B	2	828						
196	C&D	D	4		0.61	0.038	0.081	0.35	0.044	0.1
195	A(A&B)	E	4	307	0.65	0.13	0.147	0.65	0.05	0.12
197	D	D	4	332	0.619	0.05	0.244	0.112	0.047	0.2815
192	G	F	4	416						
190	G	F	4	426						
190	G	F	4	426						
190	G	F	5	426				0.58	0.058	0.1
195	C	F	5	336	0.38	0.047	0.097	0.59	0.041	0.11
193	D	F	5	601	0.21	0.031	0.081	0.43	0.044	0.11
197	A&B	C	6	3289	0.525	0.044	0.075	0.4	0.05	0.0565
196	A&B	C	6		0.66	0.056	0.069	0.54	0.053	0.063
193	A	C	6	1169						
193	A&B	D	6	1169	0.46	0.038	0.078	0.515	0.0425	0.05475
191	A	C	6	3680	0.5	0.063	0.1005	0.519	0.047	0.0515
194	A&B	A	7		0.14	0.025	0.075	0.116	0.051	0.1
194	C	A	7		0.18	0.063	0.166	0.188	0.056	0.088
194	A&B	A	7					0.194	0.031	0.056
194	A&B	A	7							